CHEMMEDCHEM

CHEMISTRY ENABLING DRUG DISCOVERY

Accepted Article

Title: Discovery of Benzimidazole Quinolone Hybrids as New Cleaving Agents towards Drug-resistant P. aeruginosa DNA

Authors: Cheng-He Zhou, Ya-Nan Wang, Rammohan R. Yadav Bheemanaboina, Wei-Wei Gao, Jie Kang, and Gui-Xin Cai

To be cited as: *ChemMedChem* 10.1002/cmdc.201700739

Link to VoR: http://dx.doi.org/10.1002/cmdc.201700739

A Journal of

ChemPubSoc Europe

WILEY-VCH

www.chemmedchem.org

Discovery of Benzimidazole Quinolone Hybrids as New Cleaving Agents towards Drug-resistant *P. aeruginosa* DNA

Ya-Nan Wang,[ξ[a]] Rammohan R. Yadav Bheemanaboina,[§[a]] Wei-Wei Gao,[§[a]] Jie Kang,[ξ[a]] Gui-Xin Cai*[a] and Cheng-He Zhou*[a]

ξ M. Sc. Y. N. Wang, M. Sc. J. Kang.
§ Dr. R. R. Y. Bheemanaboina (Postdoctoral fellow from CSIR-Indian Institute of Integrative Medicine (IIIM), India), Dr. W. W. Gao.
* A. Prof. G. X. Cai, E-mail: gxcai@swu.edu.cn, Prof. C. H. Zhou, E-mail: zhouch@swu.edu.cn (C. H. Zhou); Fax: +86-23-68254967; Tel: +86-23-68254967.
[a] Institute of Bioorganic & Medicinal Chemistry, Key Laboratory of Applied Chemistry of Chongqing Municipality, School of Chemistry and Chemical Engineering, Southwest University, Chongqing 400715, China.

Abstract: A series of benzimidazole quinolone hybrids as new potential antimicrobial agents were designed and synthesized, and their bioactive assay indicated that some prepared compounds exhibited potent antibacterial and antifungal activities. Notably, 2-fluorobenzyl derivative **5b** showed remarkable antimicrobial activities against the resistant *P. aeruginosa* and *C. tropicalis* isolated from infected patients. The active molecule **5b** could not only rapidly kill the tested strains, but also exhibit low toxicity towards Hep-2 cells. It was more difficult than norfloxacin to trigger the development of bacterial resistance against *P. aeruginosa*. Molecular docking demonstrated that it could effectively bind with topoisomerase IV–DNA complexes, and quantum chemical studies theoretically elucidated the good antimicrobial activity of compound **5b**. Preliminary experimental mechanism exploration suggested that derivative **5b** could not intercalate into DNA isolated from drug-resistant *P. aeruginosa*, but it was able to cleave DNA effectively, which might further block DNA replication to exert the powerful bioactivities. In addition, compound **5b** was found to be a promising antibacterial agent with membrane disruption ability.

Introduction

The successful discovery of quinolone antimicrobials greatly decreased the morbidity and mortality caused by fatal bacterial infections. Their good therapy effectiveness, broad antibacterial spectrum and good safety profile rapidly promoted the development of this class of antibacterial agents as first-line alternative to treat respiratory, urinary tract and bone joint infections.[1-3] Especially, the synthesis of fluoroquinolone family made great contribution to anti-infective agents such as norfloxacin, ciprofloxacin, levofloxacin and moxifloxacin.[4,5] Antimicrobial mechanism revealed that this type of drugs could target DNA gyrase or topoisomerase IV by binding with enzyme–DNA binary complexes to form ternary supramolecular complexes, thereby obstructing DNA replication and finally resulting in bacterial death.[6-8] However, the overuse of quinolones to manage bacterial infections has led to the evolution and widespread distribution of resistant strains such as *Streptococcus pneumoniae, Escherichia coli* and *Staphylococcus aureus*.[9-11] It was reported that resistance to quinolones was mainly attributed to the mutations of some key enzymes in quinolone-resistant pathogens. Particularly, the alterations in the conserved ParC helix a4 residues of topoisomerase IV–DNA complex, positioned in close proximity to the groups at *N*-1 position of quinolones, directly weakened the binding affinity between quinolone antimicrobials and target enzymes.[12,13] Accordingly, it is a promising strategy that azole rings were introduced into *N*-1 position of quinolones to strengthen the binding affinity and overcome resistance, because azole rings could bind with DNA, enzymes and receptors in organism through various weak interactions like coordination bonds, hydrogen bonds, π-π stacking and hydrophobic effect.[14-16]

Benzimidazole with a large conjugated rigid planar structure is structurally similar to purine nucleoside base, and has been arousing an increasing interest in drug design to develop potential antimicrobial agents.[17-19] Benzimidazole derivatives could interact with DNA from different microbial strains or inhibit the biosynthesis of essential ergosterol in the membrane of fungi and protozoa to exhibit the antimicrobial activities.[20,21] Previous work reported that some benzimidazole-based hybrids, such as sulfonamides, 5-fluorouracils and naphthalimides, exhibited good antimicrobial activities and broad antibacterial spectrum.[22] Biochemical and pharmacological studies showed that the modification of benzimidazole nucleus at *N*-1 and *C*-2 positions could effectively improve the bioactivity and attracted considerable attention.[23,24] All these findings clearly demonstrated a large potentiality for benzimidazole compounds in treating microbial infection.

A great deal of literature has reported that some aromatic azoles in combination with quinolones displayed good antibacterial efficacies, especially towards some drug-resistant bacteria like methicillin-resistant *Staphylococcus aureus* (MRSA) with strong activity and low toxicity.[25-27] However, to our best knowledge, the combination of benzimidazole and the quinolone backbone, especially at *N*-1 position has been seldom observed. In view of the above mentioned and as an extension of our previous work,[28] herein a series of novel benzimidazole quinolone hybrids were designed through the introduction of benzimidazole moiety to *N*-1 position of quinolones using methylene as a bridge, which allowed the flexible rotation of benzimidazole ring (Figure 1). It is expected that these hybrids would have large potentiality in the treatment of bacteria-infected diseases. The halogen atoms on quinolone skeleton may increase protein-ligand stability, and subsequently contribute to the binding affinity.[29] Various substituents including aliphatic chains and aralkyl groups were introduced to *N*-1 position of benzimidazole nucleus to investigate their effects on antimicrobial activities since substituents in *N*-position of azoles could significantly influence the pharmacological properties by regulating lipid-water partition coefficient and binding affinity.[30,31] All target molecules would be screened against Gram-positive bacteria, Gram-negative bacteria and fungal strains. To evaluate the potentiality of the most active compound as a new antibacterial candidate, further researches including partition coefficient

calculation, bacterial resistance assay, time-kill kinetic and cytotoxicity evaluation were carried out to predict its pharmacokinetic behaviors. Moreover, ligand-receptor docking was undertaken to rationalize the antibacterial activity and understand the possible action mechanism. The structural parameters such as molecular orbital energy and electrostatic potential were also computed to demonstrate the structure essential for antimicrobial activity. In addition, preliminary interaction with DNA isolated from the sensitive strains and bacterial membrane was investigated to explore the possible antimicrobial action mechanism.[32,33]

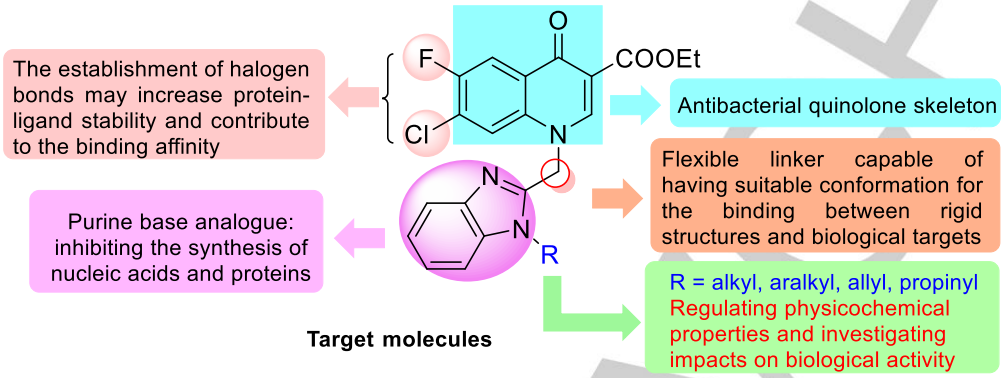

Figure 1. Design of novel benzimidazole quinolone hybrids.

Results and Discussion

Chemistry

The target benzimidazole quinolones **4–6** were synthesized *via* multi-step reactions from commercially available diethyl malonate, 3-chloro-4-fluoroaniline and *o*-phenylenediamine. The synthesis was outlined in Schemes 1–2. Diethyl 2-(ethoxymethylene)malonate **1** was easily prepared by the condensation of diethyl malonate and triethyl orthoformate with acetic anhydride, and then was reacted with 3-chloro-4-fluoroaniline using ethanol as solvent to produce diethyl intermediate **2** in 85% yield. The further cyclization of compound **2** in phenoxybenzene under reflux formed the desired 1,4-dihydroquinoline derivative **3** in moderate yield (58%). The benzimidazole quinolone hybrids **4–6** were prepared by the coupling of quinolone **3** with a series of *N*-substituted chloromethyl benzimidazoles **8**, **10** and **12** in acetonitrile with yields ranging from 25% to 52% (Scheme 1). Intermediates **8**, **10** and **12** were prepared in 74–83% yields from the cyclization of *N*-mono substituted *o*-phenylenediamines with chloroacetic acid in hydrochloric acid at reflux. The mono-substituted *o*-phenylenediamines **7**, **9** and **11** were obtained in yields of 62–69% by the nucleophilic substitution of *o*-phenylenediamine with a series of alkyl halides, benzyl halides and 3-bromoprop-1-ene/3-bromoprop-1-yne at a ratio of 1.2 : 1 (Scheme 2). All the new compounds were confirmed by ^{1}H NMR, ^{13}C NMR, IR and HRMS spectra and their spectral data were provided in the Experimental Section.

Biological activity

The antimicrobial activities *in vitro* for all the target compounds were evaluated for five Gram-positive bacteria (Methicillin-Resistant *Staphylococcus aureus* N315 (MRSA), *Enterococcus faecalis*, *Staphylococcus aureus*, *Staphylococcus aureus* ATCC 25923 and *Staphylococcus aureus* ATCC 29213), six Gram-negative bacteria (*Klebsiella pneumonia*, *Escherichia coli*, *Pseudomonas aeruginosa*, *Acinetobacter baumanii*, *Pseudomonas aeruginosa* ATCC 27853, *Escherichia coli* ATCC 25922) and five fungi (*Candida albicans*, *Candida tropicalis, Aspergillus fumigates*, *Candida albicans* ATCC 90023, *Candida parapsilosis* ATCC 22019) using two folds serial dilution technique in 96–well micro-test plates recommended by Clinical and Laboratory Standards Institute (CLSI)[34] with the positive control of clinically antimicrobial drugs norfloxacin, clinafloxacin and fluconazole. The antibacterial and antifungal data were summarized in Tables 1–2.

Antibacterial activity

As depicted in Table 1, some prepared compounds exhibited better antibacterial activities *in vitro* against the tested stains than norfloxacin and clinafloxacin. The 2-fluorobenzyl derivative **5b** displayed relatively efficient antibacterial activities in comparison with other benzimidazole quinolone hybrids. Especially towards *P. aeruginosa*, compound **5b** gave a quite low MIC of 1 μg/mL, which was 4- and 32-fold more potent than reference drugs norfloxacin and clinafloxacin. Furthermore, MRSA and *S. aureus* were also sensitive to compound **5b** (MIC = 8 μg/mL) comparable to norfloxacin. Moreover, this compound displayed better inhibition activity against *K. pneumonia* (16 μg/mL) than the two reference drugs. These results indicated that hybrid **5b** was worthy to be further investigated as promising antimicrobial candidate.

The structure activity relationship suggested that the length of aliphatic chain at 1-position of benzimidazole had noticeable

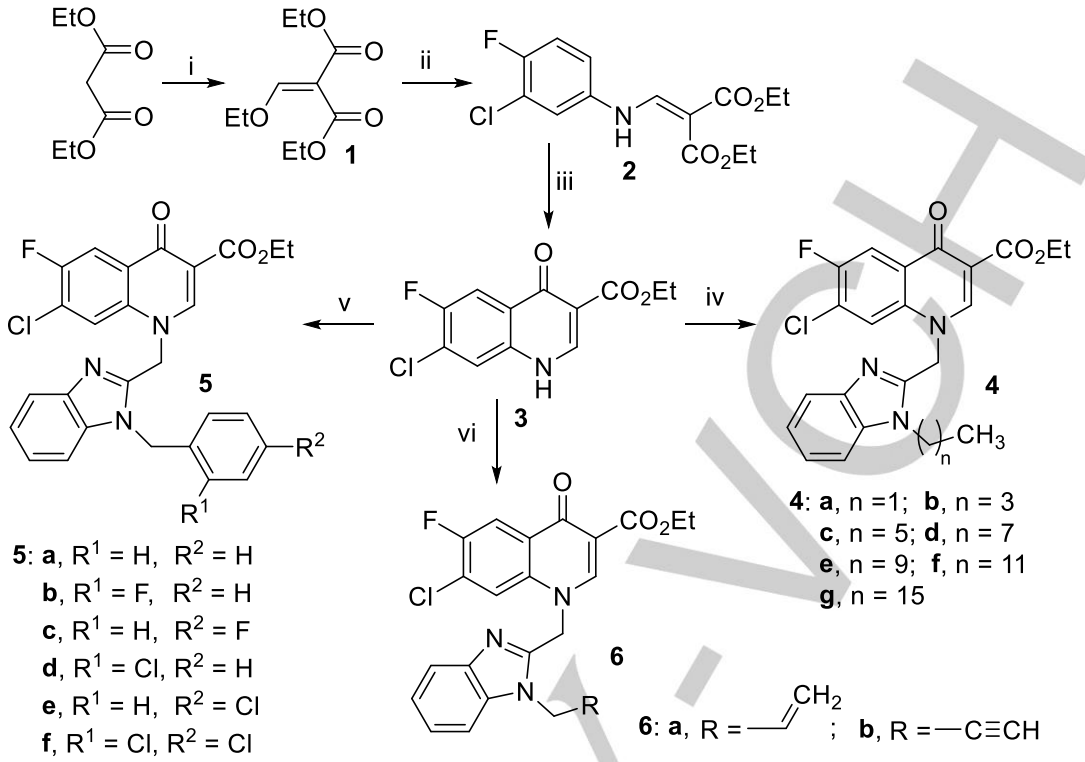

Scheme 1. Synthetic route of benzimidazole quinolone hybrids **4**, **5** and **6**. Reagents and conditions: (i) triethyl orthoformate, acetic anhydride, $ZnCl_2$, 130 °C; (ii) 3-chloro-4-fluoroaniline, 80 °C, ethanol, reflux; (iii) phenoxybenzene, 250 °C, reflux; (iv) benzimidazoles **8a–g**, potassium carbonate, acetonitrile, 70 °C; (v) benzimidazoles **10a–f**, potassium carbonate, acetonitrile, 70 °C; (vi) benzimidazoles **12a–b**, potassium carbonate, acetonitrile, 70 °C.

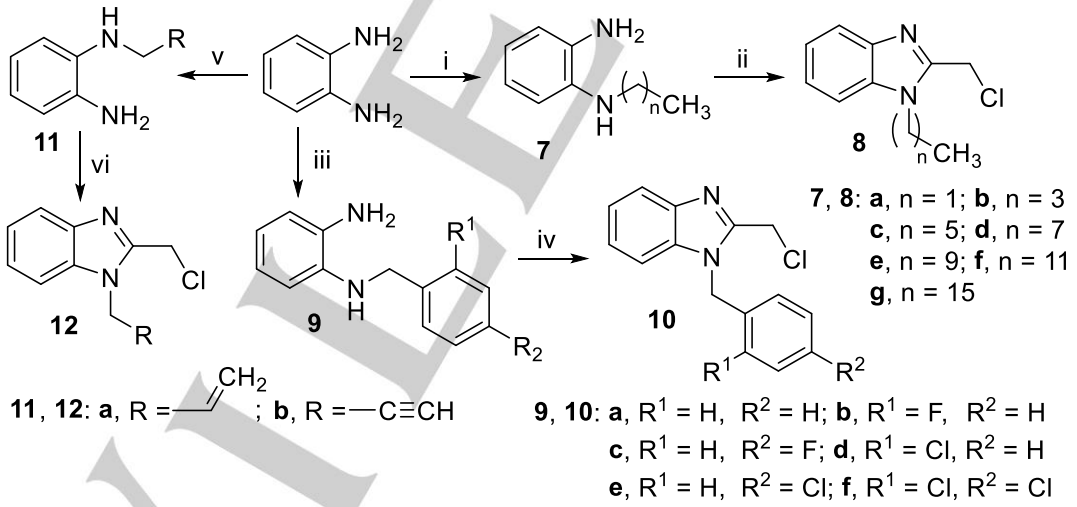

Scheme 2. Synthetic route of intermediate benzimidazoles **8**, **10** and **12**. Reagents and conditions: (i) alkyl bromide, potassium carbonate, dimethylformamide, r.t.; (ii) chloroacetic acid, 3 mol/L hydrochloric acid, reflux; (iii) halobenzyl halide, potassium carbonate, acetonitrile, 60 °C; (iv) chloroacetic acid, 6 mol/L hydrochloric acid, reflux; (v) 3-bromoprop-1-ene/ 3-bromoprop-1-yne, potassium carbonate, dimethylformamide, r.t.; (vi) chloroacetic acid, 3 mol/L hydrochloric acid, reflux.

effect on antibacterial activity. The hexyl derivative **4c** exhibited better activity against *K. pneumoniae* (MIC = 8 μg/mL) than the reference norfloxacin (MIC > 512 μg/mL). The short ethyl compound **4a** exerted more potent antibacterial activity with MIC values of 8–64 μg/mL, especially against *K. pneumoniae* (MIC = 8 μg/mL), which was 4-fold and even more active than reference drugs clinafloxacin and norfloxacin. While the replacement of ethyl group by hexadecyl chain generated compound **4g** with decreased inhibitory effects against all the tested strains (MIC > 64 μg/mL). From the overall trend of view, the increase of carbon chains had no obvious enhancement of antibacterial potency towards most of the tested strains, however, compound

4b possessed the low MIC value (8 μg/mL) against MRSA strain. These results demonstrated that the short alkyl chain might be more favourable for antibacterial activities. However, the allyl and propargyl derivatives **6a–b** displayed poor effects in suppressing bacteria, which indicated that the unsaturated aliphatic chain was not beneficial to exert inhibitory potency.

In comparison to the aliphatic derivatives **4a–g**, most of halobenzyl ones **5a–f** exerted relatively better activities in inhibiting the growth of the tested strains which might reveal that the presence of benzyl group is helpful for antimicrobial activity. The unsubstituted benzyl derivative **5a** seemed to be more sensitive towards the Gram-positive bacteria with the MIC value of 4–64 μg/mL. Fluorobenzyl compounds **5b–c** were more active than chlorobenzyl derivatives **5d–e** except for towards *E. coli* and *A. baumanii* strains. The slightly better activities for compounds **5b** and **5d** than analogs **5c** and **5e** against most of the tested strains showed that the position of halogen atoms exerted good influence in inhibiting bacterial growth. It was interesting that the antibacterial activity of compounds **5a–e** towards *S. aureus* gradually decreased and was related to the substituents of phenyl moiety. The order of activity was observed: unsubstituted phenyl **5a** > 2-fluorophenyl **5b** > 4-fluorophenyl **5c** > 2-chlorophenyl **5d** > 4-chlorophenyl one **5e**. In particular, halophenyl compound **5f** with the two chloro atoms displayed fairly good inhibition activities towards *S. aureus* (MIC = 4 μg/mL) in comparison with mono-substituted ones.

In terms of the activity against *P. aeruginosa*, the phenyl and unsaturated derivatives (**5a–f**, **6a–b**) exhibited better potency than saturated alkyl ones (**4a–g**) implying the low affinity of saturated chains. It was noticeable that all target compounds showed better activities against MRSA than reference drugs norfloxacin and clinafloxacin which suggested the potentiality of benzimidazole quinolone hybrids as anti-MRSA agents. As described above, the suitable side chain was pivotal to develop better antibacterial activities in drug design.

Table 1. Antibacterial data as MIC (μg/mL) for target compounds **4a–g**, **5a–f** and **6a–b**.[a,b,c]

Compds	Gram-positive bacteria					Gram-negative bacteria					
	MRSA	*E. faecalis*	*S. aureus*	*S. aureus* ATCC25923	*S. aureus* ATCC29213	*K. pneumoniae*	*E. coli*	*P. aeruginosa*	*A. baumanii*	*P. aeruginosa* ATCC27853	*E. coli* ATCC25922
4a	16	8	32	64	64	8	32	64	64	16	64
4b	8	32	32	128	512	8	256	512	128	256	256
4c	16	16	256	256	128	8	128	256	256	512	256
4d	64	512	64	>512	512	64	128	512	512	128	128
4e	64	256	128	512	256	256	64	256	512	256	256
4f	16	512	4	256	512	128	256	256	256	512	256
4g	128	256	64	128	256	256	256	256	128	256	128
5a	64	32	4	64	64	4	256	4	256	512	512
5b	8	64	8	64	32	16	128	1	128	32	64
5c	128	16	64	128	128	4	256	16	128	32	64
5d	64	256	128	128	256	64	256	8	128	256	128
5e	256	256	256	128	256	256	128	32	128	>512	512
5f	8	512	4	512	128	8	512	4	512	512	512
6a	8	64	128	128	64	64	128	32	64	64	64
6b	128	32	512	256	8	128	512	32	64	512	512
A	>512	2	0.5	0.5	0.5	32	64	32	8	32	0.5
B	>512	256	64	32	8	>512	512	4	32	512	1

[a] Minimum inhibitory concentrations were determined by micro broth dilution method for microdilution plates and MICs was completely inhibited concentration.
[b] MRSA, Methicillin-Resistant *Staphylococcus aureus* N315; *E. faecalis*, *Enterococcus faecalis*; *S. aureus*, *Staphylococcus aureus*; *S. aureus* ATCC25923, *Staphylococcus aureus* ATCC25923; *S. aureus* ATCC29213, *Staphylococcus aureus* ATCC29213; *K. pneumonia*, *Klebsiella pneumonia*; *E. coli*, *Escherichia coli*; *P. aeruginosa*, *Pseudomonas aeruginosa*; *A. baumanii*, *Acinetobacter baumanii*; *P. aeruginosa* ATCC27853, *Pseudomonas aeruginosa* ATCC27853; *E. coli* ATCC25922, *Escherichia coli* ATCC25922.
[c] A = Clinafloxacin, B = Norfloxacin.

Antifungal activity

The antifungal evaluation results were shown in Table 2. All benzimidazole quinolone hybrids possessed comparative even better antifungal efficiency (MIC = 1–256 μg/mL) against the clinical drug-resistant *C. tropicalis* in contrast to fluconazole (MIC = 256 μg/mL), especially compound **5b** (MIC = 1 μg/mL), which was 256-fold more active than fluconazole. Furthermore, target molecule **5b** also exhibited good inhibition potency towards *C. parapsilosis* (ATCC 22019) (MIC = 1 μg/mL) while fluconazole possessed the higher MIC value (2 μg/mL).

Alkyl substituted derivatives **4a–g** displayed moderate antifungal efficacy against most of the tested fungi, especially compounds **4a** and **4b** with the same MIC value (16 μg/mL) exhibited better activity against *C. tropicalis* than fluconazole. In addition, the unsaturated allyl or propargyl derivatives **6a–b** also showed moderate antifungal activities against most of the tested fungal strains. It was also found that fluorobenzyl compounds **5b–c** gave equivalent or even stronger antifungal activities in comparison to chlorobenzyl compounds **5d–e** against the tested strains, which indicated that fluorine atom on the phenyl moieties exerted positive effect on microbial inhibition. Probably because fluorine atom could easily and efficiently form non-covalent forces thereby being helpful for the biological transportation and distribution in organism. Dichlorophenyl compound **5f** showed lower MIC value of 16 μg/mL than monochlorophenyl ones **5d–e** (MIC = 256 μg/mL) against *C. tropicails*. On the whole, the target molecules exerted weaker antifungal activities against the other tested strains in comparison with *C. tropicails*.

Table 2. Antifungal data as MIC (μg/mL) for compounds **4a–g**, **5a–f** and **6a–b**.[d,e]

Compds	Fungi				
	C. albicans	*C. tropicalis*	*A. fumigatus*	*C. albicans* ATCC90023	*C. parapsilosis* ATCC22019
4a	256	16	64	128	64
4b	512	16	128	128	128
4c	512	128	256	256	128
4d	512	64	256	256	256
4e	256	256	128	128	128
4f	256	256	512	256	64
4g	32	256	256	256	128
5a	512	4	256	256	8
5b	256	1	256	128	1
5c	256	64	128	64	64
5d	256	256	256	128	128
5e	512	256	128	16	512
5f	512	16	256	512	128
6a	128	64	128	32	128
6b	512	128	128	64	256
C	64	256	256	1	2

[d] *C. albicans*, *Candida albicans*; *C. tropicalis*, *Candida tropicalis*; *A. fumigatus*, *Aspergillus fumigatus*; *C. albicans* ATCC90023, *Candida albicans* ATCC90023; *C. parapsilosis* ATCC22019, *Candida parapsilosis* ATCC22019.
[e] C = Fluconazole.

Effect of Clog*P* values on antimicrobial activity

Lipophilicity/hydrophilicity dominates various biological processes like the transportation, distribution, metabolism and secretion of biological molecules. A good knowledge of the lipophilicity/hydrophilicity is essential to predict the transportation and activity of drugs.[35] The partition coefficient (log*P* value) is used to define the lipophilic character of a drug, and the suitable values would have advantages in ideal pharmacokinetic and pharmacodynamic properties of drugs. Therefore, we theoretically calculated the log*P* values (Clog*P*) of all the target molecules by the commercial ChemBioOffice 2014 (Cambridge Soft, Massachusettes, USA) to further study their physical and chemical properties. As shown in Table 3, the Clog*P* values of the quinolone benzimidazole derivatives were related with the length, saturation of carbon chain and the number of fluorine and chlorine atoms in the phenyl groups. A suitable Clog*P* value exerted significant effect on antimicrobial activities. It was found that Clog*P* values in the range of 4–6 exhibited more benefits to the biological activity and higher lipophilic compounds were unfavorable which manifested the significant role of suitable lipophilicity in drug design. In general, compounds **4a–g**, **5a–f** and **6a–b** had suitable lipophilicity in comparison to clinafloxacin, norfloxacin and fluconazole which was favorable for them to permeate through biological membrane and to be delivered to the binding sites.

Table 3. Clog*P* values of compounds **4a–g**, **5a–f** and **6a–b**.[a]

Compds	Clog*P*	Compds	Clog*P*	Compds	Clog*P*
4a	4.26	**4g**	11.67	**5f**	6.68
4b	5.32	**5a**	5.25	**6a**	4.51
4c	6.38	**5b**	5.39	**6b**	3.83
4d	7.44	**5c**	5.39	**A**	-0.73
4e	8.49	**5d**	5.96	**B**	-0.78
4f	9.55	**5e**	5.96	**C**	-0.44

[a] A = Clinafloxacin, B = Norfloxacin, C = Fluconazole.

Bacterial resistance study

With the increasing development and abuse of the antibiotics, drug resistance to bacteria is inevitable. Nowadays, the study on drug resistance has become one of the most important clinical trials and the high-level resistance of norfloxacin to *P. aeruginosa* strains has been observed. Thus, the ability of *P. aeruginosa* to develop drug resistance was checked against the most potent compound **5b** and norfloxacin was used as a positive control. We exposed a standard strain of *P. aeruginosa* towards increasing concentrations of compound **5b** from sub-MIC for sustained passages. The new MIC values were tested every 24 h after propagation of *P. aeruginosa* cultures with fresh media at 37 ^{o}C on a shaker bed and serially diluted concentrations of the tested compound **5b**. The experiment was repeated for 16 days. Results in Figure 2 revealed that bacterial resistance to compound **5b** did not emerge during 12 passages in the presence of compound **5b** (1 μg/mL), and the MIC values just changed between 1 μg/mL and 4 μg/mL. However, *P. aeruginosa* developed obvious resistance to norfloxacin and the MIC values showed gradual increasing after 5 passages. This assay indicated that compound **5b** was more difficult to develop resistance against *P. aeruginosa* than clinical norfloxacin.

Bactericidal kinetic assay

In order to determine the antibacterial potency of the synthesized compounds, the viability of exponentially growing *P. aeruginosa* against highly active compound **5b** was examined by time-kill kinetics experiment. As can be seen from Figure 3, it indicated more than 1 log (CFU/mL) reduction in the number of viable bacteria within two hours at a concentration of 4 × MIC while reference drug norfloxacin underwent three hours. After three hours, the bactericidal effect of the two drugs tends to be stable. The experimental result showed that this compound had a rapid killing effect against *P. aeruginosa*.

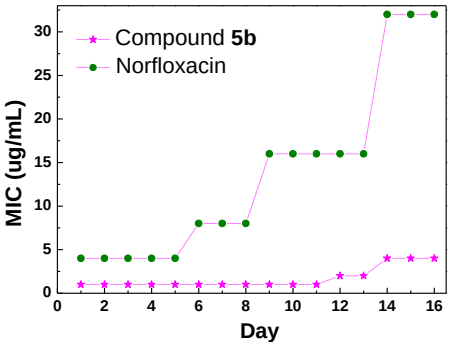

Figure 2. Evaluation of resistance development against compound **5b** in *P. aeruginosa* strains.

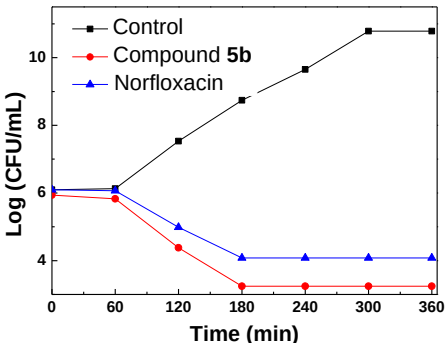

Figure 3. Time-kill kinetics of compound **5b** (4 × MIC) against *P. aeruginosa*. The data obtained are from three independent experiments performed in triplicate.

Cytotoxicity

The active molecule **5b** was further evaluated for its toxicity *in vitro* against human laryngeal carcinoma epithelial cells (Hep-2) by the colorimetric cell proliferation MTT assay. Experimental results revealed that the cell viability of Hep-2 cell against compound **5b** was more than 84%, which suggested that this molecule showed low toxicity to the cells at concentrations below 500 µg/mL and the strongest cell viability was at 300 µg/mL concentration of compound **5b** (Figure 4). All demonstrated that compound **5b** possessed the benign biocompatibility which is considered to be one of the most important properties for active drug candidates.

Molecular docking study

To rationalize the observed antibacterial activity and understand the possible action mechanism of the benzimidazole quinolone hybrids, a flexible ligand–receptor docking investigation was undertaken. The crystal structure data (topoisomerase IV–DNA complex) were obtained from the protein data bank (PDB code: 2XKK), which was representative target to investigate the antibacterial mechanism.[36] Topoisomerase IV is essential to the bacterial cell which primarily unknots and untangles DNA and is required for chromosome segregation. It alters DNA topology by generating a double-stranded break in the genetic material and passing a separate double helix through the transient DNA gate. Therefore, the active molecule **5b** was selected to dock with the topoisomerase IV–DNA complex.

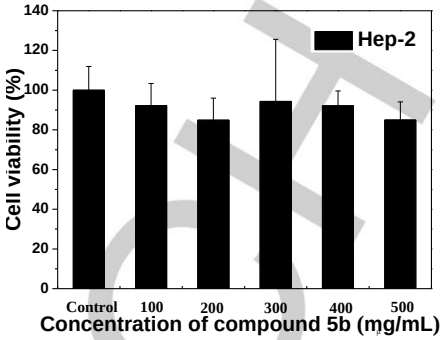

Figure 4. Cytotoxicity assay with compound **5b** in the Hep-2 cell line tested by MTT methodology. Each data bar is an average of five replicates.

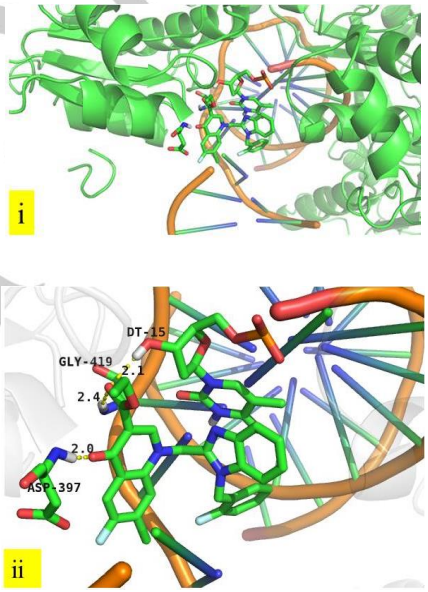

Figure 5. (i) Stereoview of conformation of compound **5b** docked in topoisomerase IV–DNA complex. (ii) Three-dimensional conformation of compound **5b** docked in topoisomerase IV–DNA complex.

Interaction of compound **5b** with topoisomerase IV–DNA receptor was shown in Figure 5 (i–ii). The docking result of target compound **5b** with topoisomerase IV–DNA complex might rationalize the possible antibacterial mechanism. The carbonyl group at 4-position of this molecule was in close vicinity to the residue Asp397 of the topoisomerase IV–DNA complex and formed hydrogen bonds. The prepared molecule **5b** could also interact with the residue Gly419 of topoisomerase IV–DNA complex and base DT15 of DNA through hydrogen bonds with distance of 2.4 and 2.1 Å, respectively through the oxygen atom of ester group. These noncovalent interactions with DNA base might block DNA replication. So, the above results showed that this cooperative binding might be propitious to stabilize the quinolone–enzyme–DNA ternary complexes which enabled compound **5b** to possess the strong inhibitory efficacy against *P. aeruginosa*. Because clinafloxacin exposes severe side effects such as phototoxicity and photohemolysis, these benzimidazole

quinolones are valuable for being further developed as potential candidates for infective chemotherapy.

Inhibitory activity against topoisomerase IV

To investigate inhibitory activity against the target enzyme of quinolones at a molecular level, compound **5b** and norfloxacin were selected to test their inhibitory activity against topoisomerase IV. Table 4 showed that compound **5b** could inhibit the activity of topoisomerase IV with a low IC_{50} value of 9.64 μM, which gave better inhibitory potency than the standard drug norfloxacin (IC_{50} = 13.48 μM).

Table 4. Inhibitory activity of compound **5b** against topoisomerase IV.

Compds	Topoisomerase IV (IC_{50}, μM)
5b	9.64
norfloxacin	13.48

Quantum chemical studies

It is known that intermolecular interactions were dominated by the frontier molecular orbital (FMO), namely the highest occupied molecular orbital (HOMO) and the lowest unoccupied molecular orbital (LUMO).[37] A detailed knowledge of the molecular electron density distribution and the electronic motion are indispensable to understand the molecular recognition and chemical reactivity of the molecule. Therefore, the concept extends into drug–receptor binding systems and the major contribution to binding involves the interaction between the HOMO of the drug with the LUMO of the receptor and that between LUMO of the drug with the HOMO of the receptor. The extents of these stabilizing interactions are inversely related to the energy gap between the interacting orbitals. Higher HOMO energy and lower LUMO energy in the drug molecule result in larger stabilizing interactions. Hence, the orbital energies of both HOMO and LUMO and their gaps were calculated for compounds **4a**, **5b** and **6a** as shown in Table 5. The HOMO-LUMO energy gap value supports the intramolecular charge-transfer interactions within the molecule. It was noteworthy that the most active compound **5b** gave rise to the lowest energy gap (Δε) of 4.56 eV.

Table 5. Energies of both HOMO and LUMO and their gaps (in eV) calculated for compounds **4a**, **5b** and **6a**.

Compds	ε HOMO (eV)	ε LUMO (eV)	Δε (eV)
4a	-6.27	-1.66	4.61
5b	-6.12	-1.56	4.56
6a	-6.23	-1.63	4.60

The plots of HOMOs and LUMOs for **4a**, **5b** and **6a** were also obtained successfully to further analyze the main atomic contributions for these orbitals. The results presented in Table 6 demonstrated that the electron charge cloud is located at the quinolone ring in highest occupied molecular orbital (HOMO) of compounds **4a**, **5b** and **6a** which indicated that active sites might be at this ring and biological interactions could take place between positively charged molecules and these sites. It was also found that benzimidazole ring and substituents on the ring did not contribute directly to HOMOs which manifested these groups might be primarily used to modulate the physicochemical properties. Moreover, the LUMOs of these molecules were also mainly centered at the quinolone ring in which nucleophilic attacks might be favorable. In order to further understand the lower antimicrobial activities of compounds **4a** and **6a** together with the higher antimicrobial activity of **5b**, molecular electrostatic potentials (MEPs) have been proceeded to check the similarities and differences in electrostatic binding characteristic of the surface of the molecules (Table 6). Comparison of the electrostatic maps of compounds **4a**, **5b** and **6a** revealed that compound **5b** had a decreased positive charge region (blue region) located on the benzimidazole ring probably due to influence of the aromatic substituent, while **5b** possessed more negative charge region (red region) on the oxygen atom of quinolone ring. It might indicate that compound **5b** had strong capability of interacting with positively charged polar residues of enzymes or receptors to form hydrogen bond through the oxygen atom of quinolone ring. This was consistent with the binding mode obtained from above docking study (Figure 5).

Interactions with drug-resistant *P. aeruginosa* DNA

It is well known that DNA, a significant information molecule encoding the genetic instructions, was commonly applied to develop almost all the known living organisms. Interestingly, it has been taken as the main cellular target to study bioactive small molecules which was conducive to designing and preparing new and efficient drugs.[38] We isolated genomic DNA from *P. aeruginosa* bacterial strain (Figure S4, supporting information). The interaction of *P. aeruginosa* DNA with the active compound **5b** was investigated by UV–vis spectroscopy to further explore the preliminary antimicrobial mechanism. The purity of DNA was checked by UV–vis spectroscopic method (Figure S1, supporting information) and the ratio of the absorbance at 260 nm to that at 280 nm was monitored. The solution gave a ratio of > 1.8 at A260/A280, which indicated that the DNA was sufficiently free from protein.

Absorption spectra of drug-resistant *P. aeruginosa* DNA in the presence of compound 5b

The investigation of DNA-binding with drug molecules was directly related to absorption spectroscopy technique. In an attempt to distinguish the change of DNA double-helical structure, hypochromism and hyperchromism are very momentous spectral features in absorption spectroscopy.[39] Because of the strong interaction between the electronic states of intercalating chromophore and that of the DNA bases, the observed large hypochromism strongly suggests a close proximity of the aromatic chromophore to the DNA bases.
With a fixed concentration of DNA, UV–vis absorption spectra were detected with the increasing concentration of compound **5b**. As shown in Figure 6, UV–vis spectra indicated that the maximum absorption peak of DNA at 260 nm was gradually enhanced along with a slightly red shift with the proportional addition of compound **5b** which was different from compound **5b** alone (Figure S2, supporting information). Meanwhile, spectral data displayed that the absorption value of simply sum of free DNA and free compound **5b** was a little greater than the

measured value of **5b**–DNA complex which revealed a weak hypochromic effect existed between DNA and compound **5b**. This hypochromic effect on the spectra of **5b**–DNA complex and the slight red shift may be resulted from the charge attraction of the prepared molecule **5b** to DNA base eventually provide convincing evidence of forming binary complexes. Moreover, the intercalation of the aromatic fragment of compound **5b** into the helix and the strong overlap of π-π* states in the large π-conjugated system with the electronic states of DNA bases were in accordance with the observed spectral changes.

In view of variations in the absorption spectra of DNA upon binding to **5b**, equation (1) can be applied to calculate the binding constant (K).

$$\frac{A^0}{A - A^0} = \frac{\xi_C}{\xi_{D-C} - \xi_C} + \frac{\xi_C}{\xi_{D-C} - \xi_C} \times \frac{1}{K[Q]} \qquad (1)$$

A^0 and A denote the absorbance of DNA in the absence and presence of compound **5b** at 260 nm, ξ_C and ξ_{D-C} represent the absorption coefficients of compound **5b** and compound **5b**–DNA complex respectively. The plot of $A^0/(A–A^0)$ versus 1/[compound **5b**] is formed by using the absorption titration data and linear fitting (Figure 7), producing the binding constant, K = 3.0 × 10^5 L/mol, R = 0.997, SD = 0.024 (R is the correlation coefficient, SD is standard deviation).

Table 6. Plots of the HOMO, LUMO and MEPs of compounds **4a**, **5b** and **6a**.

Compds	Optimized structure	HOMO	LUMO	MEPs
4a	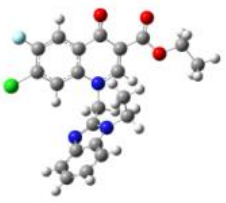		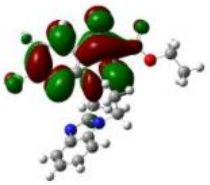	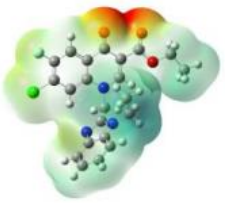 -8.000e-2
5b		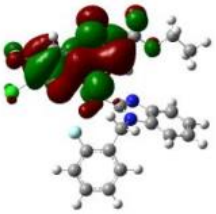		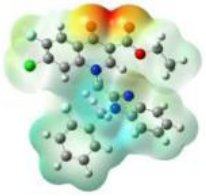 
6a				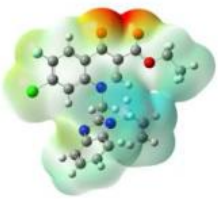 8.000e-2

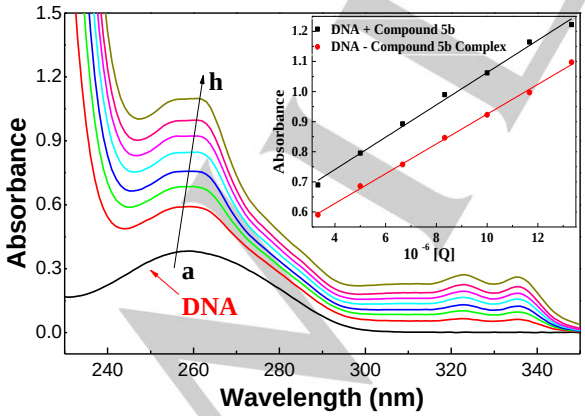

Figure 6. UV absorption spectra of DNA with different concentrations of compound **5b** (pH = 7.4, T = 290 K). Inset: comparison of absorption at 260 nm between the compound **5b**–DNA complex and the sum values of free DNA and free compound **5b**. c(DNA)= 7.44 × 10^{-5} mol/L, and c(compound **5b**) = 3.33–13.33 × 10^{-6} mol/L for curves *b*–*h* respectively at increment 1.67 × 10^{-6}.

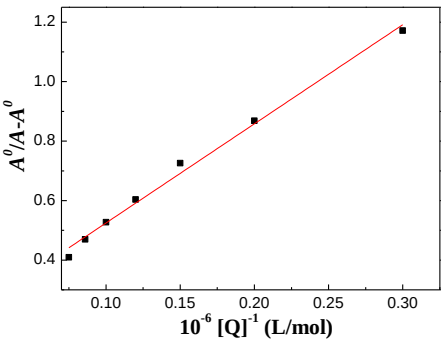

Figure 7. The plot of $A^0/(A\text{-}A^0)$ versus 1/[compound **5b**].

Absorption spectra of NR interaction with drug-resistant *P. aeruginosa* DNA

To learn more about the interaction between compound **5b** and DNA, the absorption spectra of competitive interaction of compound **5b** was investigated. Neutral Red (NR) is a planar

phenazine dye and has been widely employed as probe due to its lower toxicity, higher stability and more convenient application than other common probes. Furthermore, spectrophotometric and electrochemical techniques have already sufficiently demonstrated that NR can bind with DNA through an intercalative mode.[40] Therefore, NR was used as a spectral probe to study the binding mode of **5b** with DNA in our work. The absorption spectra of the NR dye upon the addition of DNA are shown in Figure 8. Experimental results displayed that the absorption peak of the NR around 460 nm gradually decreased with increasing concentration of DNA and a new band at around 530 nm developed, which suggested the formation of new DNA–NR complex (Figure 8). An isosbestic point at 504 nm provided evidence of DNA–NR complexformation.

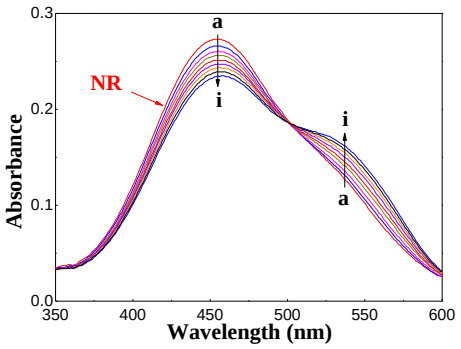

Figure 8. UV absorption spectra of NR in the presence of DNA at pH 7.4 and room temperature. c(NR) = 2 × 10^{-5} mol/L, and c(DNA) = 0–4.32 × 10^{-5} mol/L for curves *a*–*i* respectively at increment 0.48 × 10^{-5} mol/L.

Absorption spectra of competitive interaction of compound 5b and NR with drug-resistant *P. aeruginosa* DNA

Figure 9 displayed the absorption spectra of a competitive binding between NR and **5b** with DNA. As shown in Figure 9, with the increasing concentration of compound **5b**, an apparent intensity change was not observed in the developing band around 460 nm. Compared with the absorption around 460 nm of free NR in the presence of the increasing concentrations of DNA (Figure 8), the absorbance at the same wavelength did not exhibit the reverse process (inset of Figure 9). The results disclosed that compound **5b** failed to intercalate into the double helix of DNA by substituting for NR in the DNA–NR complex.

Cleavge of drug-resistant *P. aeruginosa* DNA

To further elucidate the antibacterial mechanism of this class of hybrids, the DNA cleavge experiment on compound **5b** was performed. Before the agarose gel electrophoresis test, the Job-Curve of compound **5b** and Cu^{2+} ion was made by UV spectral method. When the total concentration of Cu^{2+} ion and compound **5b** was fixed at 7.5 × 10^{-4} mol/L, the UV spectra were recorded by changing their mole ratios. As depicted in Figure 10, the most stable absorbance was at 0.5, meaning the concentrations of Cu^{2+} ion and compound **5b** were 2.5 × 10^{-4} mol/L and 5 × 10^{-4} mol/L respectively, which suggested that compound **5b** and Cu^{2+} ion could form complexwith the mole ratio of 2:1.

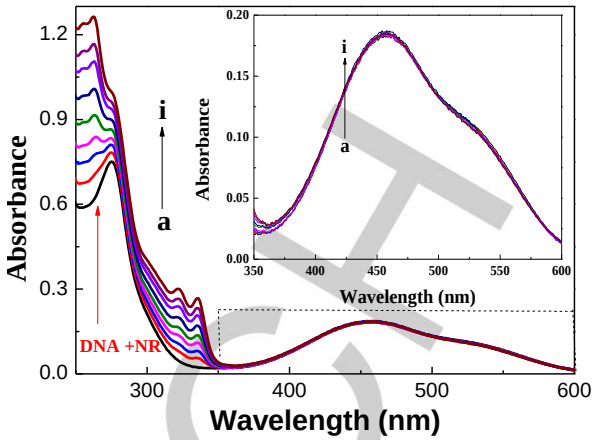

Figure 9. UV absorption spectra of the competitive reaction between compound **5b** and NR with DNA. c(DNA) = 7.44 × 10^{-5} mol/L, c(NR) = 2 × 10^{-5} mol/L, and c(compound **5b**) = 0–13.3 × 10^{-6} mol/L for curves *a*–*i* respectively at increment 1.67 × 10^{-6}. (Inset) Absorption spectra of the system with the increasing concentration of **5b** in the wavelength range of 350–600 nm absorption spectra of competitive reaction between compound **5b** and NR with DNA.

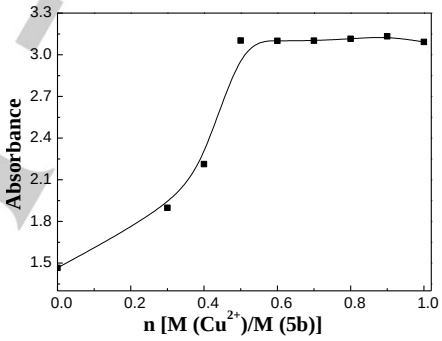

Figure 10. The Job-Curve of compound **5b** and Cu^{2+} ion; T = 298 K, λ = 229 nm, c (Cu^{2+} + 5b) = 7.5 × 10^{-4} mol/L.

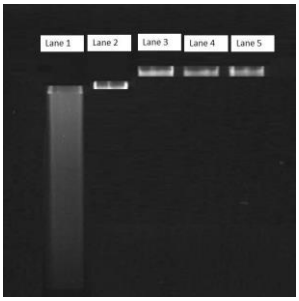

Figure 11. Agarose gel electrophoresis patterns for the cleavage of *P. aeruginosa* DNA (1.26 × 10^{-4} mol/L) by **5b**–Cu^{2+} complexes in buffer (50 mM Tris-HCl/50 mM NaCl, pH = 7.4) at 37 °C after 6 h of incubation. Lane 1, DNA + Exonuclease III enzyme(15 U/μL); Lane 2, DNA + **5b**–Cu^{2+} complexes (0.75 mM); Lane 3, DNA control; Lane 4, DNA + $Cu(NO_3)_2$ (0.75 mM); Lane 5, DNA + **5b** (0.75 mM).

The purity of *P. aeruginosa* DNA was checked by gel electrophoresis (Figure S4, supporting information). The DNA cleavage properties of **5b**–Cu^{2+} complex were confirmed in Figure 11. The experimental results manifested that compound **5b**–Cu^{2+} complex could cleave DNA effectively (Figure 11, Lane

2) in comparison with Exonuclease III enzyme as a positive control (Figure 11, Lane 1), but neither Cu^{2+} ion nor compound **5b** could cleave the *P. aeruginosa* DNA alone (Figure 11, Lane 4 and 5). Herein, it could be deduced that compound **5b** was able to form complex with Cu^{2+} ion, which might further destroy DNA directly thus enhancing its antibacterial activity. The results revealed that compound **5b** might inhibit the growth of *P. aeruginosa* by cleaving DNA, thus enhancing its antibacterial activity.

Bacterial membrane permeabilization

The ability of compound **5b** to permeabilize the bacterial cell membrane was studied using propidium iodide (PI) dye which can pass through the membrane of compromised bacterial cells and fluoresces upon binding to the cellular DNA. With the addition of compound **5b**, an enhancement in the fluorescence intensity was observed in *P. aeruginosa* within 20 minutes and then a stable trend was kept (Figure 12). Therefore, the phenomenon demonstrated that compound **5b** had the potential to permeabilize the negatively charged bacterial cell membrane of drug-resistant *P. aeruginosa* and disrupt the membrane integrity.

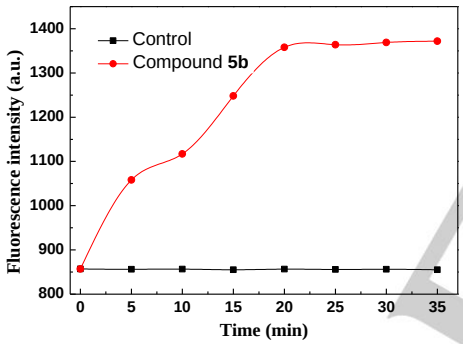

Figure 12. Bacterial membrane permeabilization of compound **5b** at concentrations of 12 × MIC against *P. aeruginosa*.

Conclusions

In conclusion, we have successfully developed a series of novel benzimidazole quinolone hybrids **4a–g**, **5a–f** and **6a–b** as potential antimicrobial agents *via* convenient and efficient synthetic procedures. All new compounds were confirmed by ^{1}H NMR, ^{13}C NMR, IR and HRMS spectra. Some of the synthesized compounds exhibited good or even superior bioactivities to reference drugs against the tested bacterial strains. The structure activity relationship found that the substituents at the *N*-position of benzimidazole ring exerted a noticeable effect on the biological activity and 2-fluorobenzyl derivative **5b** was the most prominent one. Bacterial resistance study indicated that compound **5b** was more difficult to develop resistance against *P. aeruginosa* than clinical norfloxacin and bactericidal kinetic assay showed that this compound had a rapid killing effect against *P. aeruginosa*. Moreover, the active molecule **5b** also displayed low toxicity against Hep-2 cells. Molecular docking revealed that compound **5b** could bind with topoisomerase IV–DNA complexes through hydrogen bonds among compound **5b**, Gly419 and Asp397 residues of topoisomerase IV and DT15 base of DNA. Furthermore, quantum chemical studies validated the capability of hydrogen bond formation through the oxygen atom of quinolone ring, which was consistent with the binding mode obtained from the docking result. The preliminary action mechanism investigation revealed that derivative **5b** could not intercalate into DNA isolated from drug-resistant *P. aeruginosa*, while the **5b**–Cu^{2+} complex could cleave DNA effectively, which might block DNA replication to exert the powerful bioactivities. More importantly, compound **5b** was also able to permeabilize and disrupt the cell membrane of *P. aeruginosa*. Hence, compound **5b** could open new opportunity for being developed as therapeutic agent to tackle multidrug resistant bacterial infections.

Experimental Section

General methods

Thin-layer chromatography analysis was proceeded using pre-coated silica gel plates. Melting points were detected on M5000 melting point apparatus made in Germany and were uncorrected. Fourier transform infrared spectroscopy spectra were conducted on Bruker RFS100/S spectrophotometer (Bio-Rad, Cambridge, MA, USA) using KBr pellets in the 400–4000 cm^{-1} range. ^{1}H NMR and ^{13}C NMR spectra were recorded on a Bruker AV 600 spectrometer using TMS as an internal standard. The following abbreviations were used to specify groups: Ph = phenyl, DMSO = dimethyl sulfoxide. The chemical shifts were shown in parts per million (ppm), the coupling constants (*J*) are expressed in hertz (Hz) and signals were described as singlet (s), doublet (d), triplet (t) as well as multiplet (m). The high resolution mass spectra (HRMS) were done on an IonSpec FTICR mass spectrometer. UV spectra were recorded at room temperature on a TU-2450 spectrophotometer (Puxi Analytic Instrument Ltd. of Beijing, China) equipped with 1.0 cm quartz cells. *P. aeruginosa* DNA and NR were purchased from Sigma-Aldrich (St. Louis, MO, USA). Tris, NaCl, HCl were analytical purity. Sample masses were weighed on a microbalance with a resolution of 0.1 mg. All chemicals and solvents were commercially available and were used without further purification.

Synthesis of diethyl 2-(ethoxymethylene)malonate (1)

A mixture of diethyl malonate (1 equiv), triethyl orthoformate (1.2 equiv) and acetic anhydride (2.5 equiv) was heated at 140 ^{o}C for 5 h using zinc(II) chloride as catalyst. After the reaction was completed (monitored by TLC, petroleum), the generated ethanol and acetic acid were evaporated under reduced pressure to give yellow liquid with the yield of 65%.

Synthesis of diethyl 2-(((3-chloro-4-fluorophenyl)amino) methylene)malonate (2)

Compound **1** (1 equiv) was stirred in ethanol at 80 ^{o}C for 0.5 h, and then 3-chloro-4-fluoroaniline (1 equiv) was poured into the mixture. After the reaction was completed (monitored by TLC, eluent, petroleum/ethyl acetate 20/3, V/V) about 8 h, the mixture was cooled to room temperature, and then the generated ethanol was evaporated under reduced pressure. The residue was purified *via* silica gel column chromatography (eluent, petroleum) to afford compound **2** as light yellow solid in 85% yield.[41]

Synthesis of ethyl 7-chloro-6-fluoro-4-oxo-1,4-dihydroquinoline-3-carboxylate (3)

Diphenylether (50 mL) was heated to 250 °C and then compound **2** (6.3 g, 0.02 mol) was slowly added. The mixture was refluxed for 1.5 h. When the reaction was completed (monitored by TLC, eluent, chloroform/methanol 70/1, v/v), the system was cooled to room temperature and washed with petroleum ether to remove the excess of diphenylether. The white solid was collected with 58% of yield (mp > 250 °C).

Synthesis of mono-substituted o-phenylenediamines (7, 9, 11) and chloromethyl benzimidazoles (8, 10, 12)

The intermediates **7–12** were prepared according to the literature procedure, starting from *o*-phenylenediamine.[12,42]

Synthesis of ethyl 7-chloro-1-((1-ethyl-1H-benzo[d]imidazol-2-yl) methyl)-6-fluoro-4-oxo-1,4-dihydro quinoline-3-carboxylate (4a)

A mixture of compound **3** (500 mg, 1.854 mmol), potassium carbonate (256 mg, 1.854 mmol) and sodium iodide (278 mg, 1.854 mmol) in acetonitrile (10 mL) was stirred at 70 °C for 0.5 h. After the mixture was cooled to room temperature, compound **8a** (361 mg, 1.854 mmol) was added. The reaction mixture was then heated at 70 °C for 3 h. After the reaction was completed (monitored by TLC, dichloromethane/ethyl acetate (1/1, V/V)), the reaction was cooled to room temperature and treated with formic acid to adjust the pH value to 5.5–6.5. After the acetonitrile was removed under reduced pressure, the resulting mixture was purified by silica gel chromatography eluting with dichloromethane/ethyl acetate (10/1, V/V) to give the pure target compound **4a** as white solid (334 mg). Yield: 42.1%; mp: 103–104 °C; IR (KBr, cm^{-1}) v: 3044 (aromatic C–H), 2978, 2934 (CH_2, CH_3), 1725, 1694 (C=O), 1614, 1550, 1486, (aromatic frame); ^{1}H NMR (600 MHz, $CDCl_3$, ppm) δ 8.62 (s, quinolone-2-*H*, 1H), 8.13 (d, *J* = 8.9 Hz, quinolone-5-*H*, 1H), 7.90 (d, *J* = 5.5 Hz, quinolone-8-*H*, 1H), 7.72 (d, *J* = 8.0 Hz, benzimidazolyl-4-*H*, 1H), 7.38 (d, *J* = 8.0 Hz, benzimidazolyl-7-*H*, 1H), 7.33 (t, *J* = 7.5 Hz, benzimidazolyl-5-*H*, 1H), 7.30–7.27 (m, benzimidazolyl-6-*H*, 1H), 5.65 (s, quinolone-1-NCH_2, 2H), 4.36–4.32 (m, NCH_2CH$_3$, 2H), 4.30 (dd, *J* = 15.4, 8.1 Hz, COOCH_2, 2H), 1.39–1.35 (m, NCH$_2$CH_3, COOCH$_2$CH_3, 6H); ^{13}C NMR (151 MHz, $CDCl_3$, ppm) δ 172.8 (*C*=O), 164.8 (O=*C*OCH$_2$CH$_3$), 156.5 (aromatic *C*-F), 154.9, 149.5, 145.3, 142.2, 136.1, 135.1, 123.9, 123.0, 120.4, 119.30, 114.0, 113.8, 111.5, 109.7, 61.1, 51.3 (*C*H$_2$), 39.2, 15.2, 14.3; ESI-MS (m/z): 428 $[M+H]^+$; HRMS (TOF) calcd. for $C_{22}H_{19}ClFN_3O_3$ $[M+H]^+$: 428.1177; found, 428.1180.

Synthesis of ethyl 1-((1-butyl-1H-benzo[d]imidazol-2-yl)methyl)-7-chloro-6-fluoro-4-oxo-1,4-dihydroquinoline-3-carboxylate (4b)

Compound **4b** was prepared according to the procedure for the preparation of compound **4a**, starting from compound **3** (1.000 g, 3.708 mmol), potassium carbonate (512 mg, 3.708 mmol), sodium iodide (556 mg, 3.708 mmol) and compound **8b** (826 mg, 3.708 mmol). The pure product **4b** was obtained as white solid (760 mg). Yield: 44.9%; mp: 102–103 °C; IR (KBr, cm^{-1}) v: 3039 (aromatic C–H), 2973, 2954, 2929, 2873, 2852 (CH_2, CH_3), 1711, 1633 (C=O), 1613, 1551, 1487, (aromatic frame); ^{1}H NMR (600 MHz, DMSO-d_6, ppm) δ 8.94 (s, quinolone-2-*H*, 1H), 8.09 (dd, *J* = 17.9, 7.5 Hz, quinolone-5,8-*H*, 2H), 7.60 (d, *J* = 8.1 Hz, benzimidazolyl-4-*H*, 1H), 7.50 (d, *J* = 8.0 Hz, benzimidazolyl-7-*H*, 1H), 7.25 (t, *J* = 7.6 Hz, benzimidazolyl-5-*H*, 1H), 7.14 (t, *J* = 7.6 Hz, benzimidazolyl-6-*H*, 1H), 6.06 (s, quinolone-1-NCH_2, 2H), 4.36 (t, *J* = 7.6 Hz, CH_2CH$_2$CH$_2$CH$_3$, 2H), 4.25 (q, *J* = 7.0 Hz, COOCH_2, 2H), 1.82–1.71 (m, CH$_2$CH_2CH$_2$CH$_3$, 2H), 1.48–1.37 (m, CH$_2$CH$_2$CH_2CH$_3$, 2H), 1.29 (t, *J* = 7.1 Hz, COOCH$_2$CH_3, 3H), 0.96 (t, *J* = 7.3 Hz, CH$_2$CH$_2$CH$_2$CH_3, 3H); ^{13}C NMR (151 MHz, DMSO-d_6, ppm) δ 172.7 (C=O), 164.5 (O=*C*OCH$_2$CH$_3$), 156.0 (aromatic C-F), 154.4, 151.8, 148.9, 137.2, 129.3, 129.3, 126.1, 120.2, 118.3, 116.4, 114.5, 113.0, 112.6, 112.1, 60.5, 48.8 (*C*H$_2$), 45.5, 30.6, 20.0, 14.5, 13.7; ESI-MS (m/z): 456 $[M+H]^+$; HRMS (TOF) calcd. for $C_{24}H_{24}ClFN_3O_3$ $[M+H]^+$: 456.1490; found, 456.1492.

Synthesis of ethyl 7-chloro-6-fluoro-1-((1-hexyl-1H-benzo[d]imidazol-2-yl)methyl)-4-oxo-1,4-dihydroquinoline-3-carboxylate (4c)

Compound **4c** was prepared according to the procedure for the preparation of compound **4a**, starting from compound **3** (2.000 g, 7.417 mmol), potassium carbonate (1.024 g, 7.417 mmol), sodium iodide (1.112 g, 7.417 mmol) and compound **8c** (1.860 g, 7.417 mmol). The pure product **4c** was obtained as white solid (1.867 g). Yield: 52.0%; mp: 104–105 °C; IR (KBr, cm^{-1}) v: 3046 (aromatic C–H), 2956, 2931, 2858 (CH_2, CH_3), 1724, 1682 (C=O), 1636, 1613, 1550, 1486, (aromatic frame); ^{1}H NMR (600 MHz, DMSO-d_6, ppm) δ 8.97 (s, quinolone-2-*H*, 1H), 8.17 (d, *J* = 5.6 Hz, quinolone-5-*H*, 1H), 8.11 (d, *J* = 9.1 Hz, quinolone-8-*H*, 1H), 7.96 (d, *J* = 7.7 Hz, benzimidazolyl-4-*H*, 1H), 7.65 (d, *J* = 8.2 Hz, benzimidazolyl-7-*H*, 1H), 7.54 (d, *J* = 7.0 Hz, benzimidazolyl-5-*H*, 1H), 7.49–7.43 (m, benzimidazolyl-6-*H*, 1H), 6.28 (s, quinolone-1-NCH_2, 2H), 4.54–4.48 (t, CH_2(CH$_2$)$_4$CH$_3$, 2H), 4.27 (q, *J* = 7.0 Hz, COOCH_2, 2H), 1.92 (d, *J* = 6.2 Hz, CH$_2$CH_2(CH$_2$)$_3$CH$_3$, 2H), 1.48 (d, *J* = 6.7 Hz, (CH$_2$)$_2$CH_2(CH$_2$)$_2$CH$_3$, 2H), 1.40–1.33 (m, (CH$_2$)$_3$CH_2CH_2CH$_3$, 4H), 1.29 (t, *J* = 7.0 Hz, COOCH$_2$CH_3, 3H), 0.91 (t, *J* = 6.8 Hz, (CH$_2$)$_5$CH_3, 3H); 13C NMR (151 MHz, DMSO-d_6, ppm) δ 172.6 (*C*=O), 164.6 (O=*C*OCH$_2$CH$_3$), 155.9 (aromatic *C*-F), 154.3, 151.8, 149.0, 137.3, 134.2, 129.2, 125.3, 120.5, 118.4, 116.6, 114.6, 113.0, 112.7, 112.4, 60.6, 49.0 (*C*H$_2$), 45.2, 31.3, 29.0, 26.4, 22.5, 14.7, 14.2; ESI-MS (m/z): 484 $[M+H]^+$; HRMS (TOF) calcd. for $C_{26}H_{28}ClFN_3O_3$ $[M+H]^+$: 484.1803; found, 484.1829.

Synthesis of ethyl 7-chloro-6-fluoro-1-((1-octyl-1H-benzo[d]imidazol-2-yl)methyl)-4-oxo-1,4-dihydroquinoline-3-carboxylate (4d)

Compound **4d** was prepared according to the procedure for the preparation of compound **4a**, starting from compound **3** (2.000 g, 7.417 mmol), potassium carbonate (1.024 g, 7.417 mmol), sodium iodide (1.112 g, 7.417 mmol) and compound **8d** (2.068 g, 7.417 mmol). The pure product **4d** was obtained as white solid (1.822 g). Yield: 48.0%; mp: 105–106 °C; IR (KBr, cm^{-1}) v: 3045 (aromatic C–H), 2957, 2925, 2853 (CH_2, CH_3), 1726, 1690 (C=O), 1639, 1614, 1549, 1487, (aromatic frame); ^{1}H NMR (600 MHz, $CDCl_3$, ppm) δ 8.64 (s, quinolone-2-*H*, 1H), 8.16 (d, *J* = 8.7 Hz, quinolone-5-*H*, 1H), 7.91 (d, *J* = 5.4 Hz, quinolone-8-*H*, 1H), 7.73 (d, *J* = 7.1 Hz, benzimidazolyl-4-*H*, 1H), 7.37 (d, *J* = 7.8 Hz, benzimidazolyl-7-*H*, 1H), 7.34–7.30 (t, benzimidazolyl-5-*H*, 1H), 7.28 (t, *J* = 8.8 Hz, benzimidazolyl-6-*H*, 1H), 5.65 (s, quinolone-1-NCH_2, 2H), 4.38–4.30 (t, CH_2(CH$_2$)$_6$CH$_3$, 2H), 4.20 (q, *J* = 7.4 Hz, COOCH_2, 2H), 1.70 (d, *J* = 6.6 Hz, CH$_2$CH_2(CH$_2$)$_5$CH$_3$, 2H), 1.36 (d, *J* = 6.4 Hz, (CH$_2$)$_2$CH_2CH_2(CH$_2$)$_3$CH$_3$, 4H), 1.31–1.18 (m, (CH$_2$)$_4$(CH_2)$_3$CH$_3$, COOCH$_2$CH_3, 9H), 0.86 (t, *J* = 7.0 Hz, (CH$_2$)$_7$CH_3, 3H); ^{13}C NMR (151 MHz, $CDCl_3$, ppm) δ 172.9 (*C*=O), 164.8 (O=*C*OCH$_2$CH$_3$), 156.5 (aromatic *C*-F), 154.8, 149.6, 145.7, 142.2, 136.2, 135.5, 129.2, 123.8, 122.9, 120.3, 119.3, 114.0, 111.5, 109.8, 61.0, 51.4 (*C*H$_2$), 44.6, 31.6, 30.2, 29.1, 29.1, 27.0, 22.5, 14.3, 14.0; ESI-MS (m/z): 512 $[M+H]^+$; HRMS (TOF) calcd. for $C_{28}H_{32}ClFN_3O_3$ $[M+H]^+$: 512.2116; found, 512.2123.

Synthesis of ethyl 7-chloro-1-((1-decyl-1H-benzo[d]imidazol-2-yl)methyl)-6-fluoro-4-oxo-1,4-dihydro quinoline -3-carboxylate (4e)

Compound **4e** was prepared according to the procedure for the preparation of compound **4a**, starting from compound **3** (2.000 g, 7.417 mmol), potassium carbonate (1.024 g, 7.417 mmol), sodium iodide (1.112 g, 7.417 mmol) and compound **8e** (2.271 g, 7.417 mmol). The pure product **4e** was obtained as white solid (1.642 g). Yield: 41.2%; mp: 107–108 °C; IR (KBr, cm^{-1}) v: 3053 (aromatic C–H), 2926, 2854 (CH_2, CH_3), 1888, 1724 (C=O), 1614, 1551, 1485, (aromatic frame); ^{1}H NMR (600 MHz, $CDCl_3$, ppm) δ 8.53 (s, quinolone-2-*H*, 1H), 8.06 (d, *J* = 8.9 Hz, quinolone-5-*H*, 1H), 7.79 (d, *J* = 5.4 Hz, quinolone-8-*H*, 1H), 7.64 (d, *J* = 7.9 Hz, benzimidazolyl-4-*H*, 1H), 7.27 (d, *J* = 7.9 Hz, benzimidazolyl-7-*H*, 1H), 7.24 (t, *J* = 7.4 Hz, benzimidazolyl-5-*H*, 1H), 7.19 (t, *J* = 7.3 Hz, benzimidazolyl-6-*H*, 1H), 5.54 (s, quinolone-1-NCH_2, 2H), 4.25 (q, *J* = 7.0 Hz, COOCH_2, 2H), 4.10 (t, *J* = 7.6 Hz, CH_2(CH$_2$)$_8$CH$_3$, 2H), 1.62 (dt, *J* = 15.0, 7.7 Hz, CH$_2$CH_2(CH$_2$)$_7$CH$_3$, 2H), 1.27 (t, *J* = 7.0 Hz, COOCH$_2$CH_3,

3H), 1.22–1.13 (m, $(CH_2)_2(CH_2)_7CH_3$, 14H), 0.79 (t, *J* = 7.0 Hz, $(CH_2)_9CH_3$, 3H); ^{13}C NMR (151 MHz, $CDCl_3$, ppm) δ 172.8 (*C*=O), 164.7 (O=*CO*CH_2CH_3), 156.5 (aromatic *C*-F), 154.8, 149.6, 145.7, 142.2, 136.1, 135.6, 129.1, 123.8, 122.8, 120.3, 119.3, 113.9, 111.4, 109.8, 61.0, 51.4 (CH_2), 50.6, 44.6, 31.8, 30.2, 29.4, 29.2, 29.2, 27.0, 22.6, 14.3 14.0; ESI-MS (m/z): 540 $[M+H]^+$; HRMS (TOF) calcd. for $C_{30}H_{36}ClFN_3O_3$ $[M+H]^+$: 540.2429; found, 540.2313.

Synthesis of ethyl 7-chloro-1-((1-dodecyl-1H-benzo[d]imidazol-2-yl)methyl)-6-fluoro-4-oxo-1,4-dihydro quinoline-3-carboxylate (4f)

Compound **4f** was prepared according to the procedure for the preparation of compound **4a**, starting from compound **3** (3.800 g, 14.092 mmol), potassium carbonate (1.945 g, 14.092 mmol), sodium iodide (2.112 g, 14.092 mmol) and compound **8f** (4.719 g, 14.092 mmol). The pure product **4f** was obtained as white solid (2.858 g). Yield: 35.7%; mp: 109–110 °C; IR (KBr, cm^{-1}) ν: 3054 (aromatic C–H), 2925, 2853 (CH_2, CH_3), 1920, 1725 (C=O), 1614, 1551, 1482, (aromatic frame); ^{1}H NMR (600 MHz, $CDCl_3$, ppm) δ 8.63 (s, quinolone-2-*H*, 1H), 8.10 (d, *J* = 8.9 Hz, quinolone-5-*H*, 1H), 7.83 (d, *J* = 10.3 Hz, quinolone-8-*H*, 1H), 7.68 (d, *J* = 7.6 Hz, benzimidazolyl-4-*H*, 1H), 7.35 (d, *J* = 8.0 Hz, benzimidazolyl-7-*H*, 1H), 7.30 (t, *J* = 7.5 Hz, benzimidazolyl-5-*H*, 1H), 7.26–7.24 (m, benzimidazolyl-6-*H*, 1H), 5.66 (s, quinolone-1-NCH_2, 2H), 4.30 (q, *J* = 6.9 Hz, COOCH_2, 2H), 4.20 (t, *J* = 7.6 Hz, C$H_2(CH_2)_{10}CH_3$, 2H), 1.74–1.69 (m, $CH_2CH_2(CH_2)_9CH_3$, 2H), 1.33 (t, *J* = 6.8 Hz, $(CH_2)_2CH_2(CH_2)_8CH_3$, $COOCH_2CH_3$, 5H), 1.23 (s, $(CH_2)_3(CH_2)_8CH_3$, 16H), 0.87 (t, *J* = 7.1 Hz, $(CH_2)_{11}CH_3$, 3H); ^{13}C NMR (151 MHz, $CDCl_3$, ppm) δ 172.7 (*C*=O), 164.5 (O=*CO*CH_2CH_3), 156.4 (aromatic *C*-F), 154.7, 149.7, 146.0, 142.3, 136.2, 135.6, 129.0, 123.7, 122.7, 120.3, 119.4, 113.8, 111.3, 109.8, 60.9, 51.3 (CH_2), 44.5, 31.9, 30.2, 29.5, 29.5, 29.5, 29.4, 29.3, 29.2, 27.0, 22.6, 14.3, 14.0; ESI-MS (m/z): 568 $[M+H]^+$; HRMS (TOF) calcd. for $C_{32}H_{40}ClFN_3O_3$ $[M+H]^+$: 568.2742; found, 568.2756.

Synthesis of ethyl 7-chloro-6-fluoro-1-((1-hexadecyl-1H-benzo[d] imidazol-2-yl)methyl)-4-oxo-1,4-dihydro quinoline-3-carboxylate (4g)

Compound **4g** was prepared according to the procedure for the preparationn of compound **4a**, starting from compound **3** (2.130 g, 7.899 mmol), potassium carbonate (1.090 g, 7.899 mmol) and sodium iodide (1.184 g, 7.899 mmol) and compound **8g** (3.089 g, 7.899 mmol). The pure product **4g** was obtained as white solid (1.795 g). Yield: 36.4%; mp: 114–115 °C; IR (KBr, cm^{-1}) ν: 3052 (aromatic C–H), 2924, 2853 (CH_2, CH_3), 1887, 1724 (C=O), 1614, 1551, 1486, (aromatic frame); ^{1}H NMR (600 MHz, $CDCl_3$, ppm) δ 8.60 (s, quinolone-2-*H*, 1H), 8.17 (d, *J* = 8.1 Hz, quinolone-5-*H*, 1H), 7.90 (d, *J* = 3.6 Hz, quinolone-8-*H*, 1H), 7.73 (d, *J* = 7.8 Hz, benzimidazolyl-4-*H*, 1H), 7.35 (d, *J* = 7.8 Hz, benzimidazolyl-7-*H*, 1H), 7.32 (t, *J* = 7.5 Hz, benzimidazolyl-5-*H*, 1H), 7.29 (t, *J* = 7.6 Hz, benzimidazolyl-6-*H*, 1H), 5.60 (s, quinolone-1-NCH_2, 2H), 4.36 (q, *J* = 6.6 Hz, COOCH_2, 2H), 4.17 (t, *J* = 7.5 Hz, C$H_2(CH_2)_{14}CH_3$, 2H), 1.69 (dd, *J* = 14.4, 7.3 Hz, $CH_2CH_2(CH_2)_{13}CH_3$, 2H), 1.37 (t, *J* = 6.9 Hz, $COOCH_2CH_3$, 3H), 1.24 (d, *J* = 12.8 Hz, $(CH_2)_2(CH_2)_{13}CH_3$, 26H), 0.88 (t, *J* = 6.6 Hz, $(CH_2)_{15}CH_3$, 3H); ^{13}C NMR (151 MHz, $CDCl_3$, ppm) δ 172.7 (*C*=O), 164.7 (O=*CO*CH_2CH_3), 156.5 (aromatic *C*-F), 154.9, 149.5, 145.5, 142.3, 136.1, 135.6, 129.2, 123.9, 122.9, 120.5, 119.2, 114.1, 111.5, 109.8, 61.2, 51.5 (CH_2), 50.7, 44.6, 31.9, 30.2, 29.7, 29.6, 29.6, 29.6, 29.6, 29.5. 29.4, 29.3, 29.2, 27.0, 22.6, 14.2, 14.0; ESI-MS (m/z): 624 $[M+H]^+$; HRMS (TOF) calcd. for $C_{36}H_{48}ClFN_3O_3$ $[M+H]^+$: 624.3368; found, 624.3383.

Synthesis of ethyl 1-((1-benzyl-1H-benzo[d]imidazol-2-yl)methyl)-7-chloro-6-fluoro-4-oxo-1,4-dihydro quinoline-3-carboxylate (5a)

Compound **5a** was prepared according to the procedure for the preparation of compound **4a**, starting from compound **3** (2.224 g, 8.247 mmol), potassium carbonate (1.138 g, 8.247 mmol), sodium iodide (1.236 g, 8.247 mmol) and compound **10a** (2.001 g, 8.247 mmol). The pure product **5a** was obtained as white solid (1.697 g). Yield: 42.1%; mp: 240–241 °C; IR (KBr, cm^{-1}) ν: 3056 (aromatic C–H), 2982, 2902 (CH_2, CH_3), 1727 (C=O), 1613, 1552, 1483, (aromatic frame); ^{1}H NMR (600 MHz, DMSO-d_6, ppm) δ 8.81 (s, quinolone-2-*H*, 1H), 8.02 (d, *J* = 9.2 Hz, quinolone-5-*H*, 1H), 7.95 (d, *J* = 5.8 Hz, quinolone-8-*H*, 1H), 7.58 (d, *J* = 7.9 Hz, benzimidazolyl-4-*H*, 1H), 7.50 (d, *J* = 8.1 Hz, benzimidazolyl-7-*H*, 1H), 7.30–7.26 (m, Ph-3,4,5-*H*, 3H), 7.24 (t, *J* = 7.5 Hz, benzimidazolyl-5-*H*, 1H), 7.19 (t, *J* = 7.3 Hz, benzimidazolyl-6-*H*, 1H), 7.10 (d, *J* = 6.6 Hz, Ph-2,6-*H*, 2H), 6.03 (s, quinolone-1-NCH_2, 2H), 5.70 (s, benzimidazolyl-1-NCH_2, 2H), 4.24 (q, *J* = 7.1 Hz, COOCH_2, 2H), 1.28 (t, *J* = 7.0 Hz, $COOCH_2CH_3$, 3H); ^{13}C NMR (151 MHz, DMSO-d_6, ppm) δ 172.0 (*C*=O), 164.5 (O=*CO*CH_2CH_3), 155.6 (aromatic *C*-F), 154.0, 151.3, 149.1, 142.3, 137.1, 136.6, 136.3, 129.2, 128.2, 126.9, 123.5, 122.6, 120.6, 119.7, 113.0, 112.9, 111.2, 110.9, 60.5, 50.0 (CH_2), 47.1, 14.7; ESI-MS (m/z): 490 $[M+H]^+$; HRMS (TOF) calcd. for $C_{27}H_{21}ClFN_3O_3$ $[M+H]^+$: 490.1334; found, 490.1336.

Synthesis of ethyl 7-chloro-6-fluoro-1-((1-(2-fluorobenzyl)-1H-benzo[d]imidazol-2-yl)methyl)-4-oxo-1,4-dihydro quinoline-3-carboxylate (5b)

Compound **5b** was prepared according to the procedure for the preparation of compound **4a**, starting from compound **3** (1.850 g, 6.860 mmol), potassium carbonate (0.947 g, 6.860 mmol), sodium iodide (1.028 g, 6.860 mmol) and compound **10b** (1.885 g, 6.860 mmol). The pure product **5b** was obtained as white solid (1.592 g). Yield: 45.7%; mp: 213–214 °C; IR (KBr, cm^{-1}) ν: 3040 (aromatic C–H), 2976, 2945, 2905 (CH_2, CH_3), 1704, 1634 (C=O), 1614, 1551, 1488, (aromatic frame); ^{1}H NMR (600 MHz, DMSO-d_6, ppm) δ 8.84 (s, quinolone-2-*H*, 1H), 8.09 (d, *J* = 5.7 Hz, quinolone-5-*H*, 1H), 7.99 (d, *J* = 9.2 Hz, quinolone-8-*H*, 1H), 7.61 (d, *J* = 7.8 Hz, benzimidazolyl-4-*H*, 1H), 7.50 (d, *J* = 8.0 Hz, benzimidazolyl-7-*H*, 1H), 7.30 (dd, *J* = 13.2, 6.6 Hz, FPh-3-*H*, 1H), 7.22 (dt, *J* = 11.1, 5.9 Hz, FPh-4,5,6-*H*, 3H), 6.96 (t, *J* = 7.4 Hz, benzimidazolyl-5-*H*, 1H), 6.67 (t, *J* = 7.4 Hz, benzimidazolyl-6-*H*, 1H), 6.06 (s, quinolone-1-NCH_2, 2H), 5.78 (s, benzimidazolyl-1-NCH_2, 2H), 4.23 (q, *J* = 7.0 Hz, COOCH_2, 2H), 1.28 (t, *J* = 7.1 Hz, $COOCH_2CH_3$, 3H); ^{13}C NMR (151 MHz, DMSO-d_6, ppm) δ 171.8 (*C*=O), 164.5 (O=*CO*CH_2CH_3), 161.0, 155.6, 151.1, 149.2, 142.2, 137.2, 136.3, 130.3, 128.9, 128.4, 125.1, 123.5, 122.7, 120.7, 119.8, 116.1, 115.9, 113.0, 112.8, 111.1, 110.9, 60.4, 50.1 (CH_2), 41.8, 14.7; ESI-MS (m/z): 508 $[M+H]^+$; HRMS (TOF) calcd. for $C_{27}H_{20}ClF_2N_3O_3$ $[M+H]^+$: 508.1240; found, 508.1243.

Synthesis of ethyl 7-chloro-6-fluoro-1-((1-(4-fluorobenzyl)-1H-benzo[d]imidazol-2-yl)methyl)-4-oxo-1,4-dihydro quinoline-3-carboxylate (5c)

Compound **5c** was prepared according to the procedure for the preparation of compound **4a**, starting from compound **3** (2.467 g, 9.148 mmol), potassium carbonate (1.262 g, 9.148 mmol), sodium iodide (1.371 g, 9.148 mmol) and compound **10c** (2.513 g, 9.148 mmol). The pure product **5c** was obtained as white solid (1.840 g). Yield: 39.6%; mp: 203–204 °C; IR (KBr, cm^{-1}) ν: 3053 (aromatic C–H), 2977, 2901 (CH_2, CH_3), 1894, 1711 (C=O), 1614, 1551, 1486, (aromatic frame); ^{1}H NMR (600 MHz, DMSO-d_6, ppm) δ 8.85 (s, quinolone-2-*H*, 1H), 8.03 (d, *J* = 9.2 Hz, quinolone-5-*H*, 1H), 7.99 (d, *J* = 5.7 Hz, quinolone-8-*H*, 1H), 7.58 (d, *J* = 8.0 Hz, benzimidazolyl-4-*H*, 1H), 7.52 (d, *J* = 8.0 Hz, benzimidazolyl-7-*H*, 1H), 7.24 (t, *J* = 7.5 Hz, benzimidazolyl-5-*H*, 1H), 7.18 (t, *J* = 6.4 Hz, benzimidazolyl-6-*H*, FPh-3,5-*H*, 3H), 7.12 (t, *J* = 8.7 Hz, FPh-2,6-*H*, 2H), 6.04 (s, quinolone-1-NCH_2, 2H), 5.70 (s, benzimidazolyl-1-NCH_2, 2H), 4.24 (q, *J* = 7.0 Hz, COOCH_2, 2H), 1.28 (t, *J* = 7.0 Hz, $COOCH_2CH_3$, 3H); ^{13}C NMR (151 MHz, DMSO-d_6, ppm) δ 171.9 (*C*=O), 164.6 (O=*CO*CH_2CH_3), 161.37, 155.7, 151.3, 149.2, 142.3, 137.1, 136.3, 132.9, 129.2, 129.1, 125.7, 123.5, 122.6, 120.7, 119.8, 116.1, 116.0, 113.0, 112.8, 111.1, 110.9, 60.5, 50.0 (CH_2), 46.4, 14.7; ESI-MS (m/z): 508 $[M+H]^+$; HRMS (TOF) calcd. for $C_{27}H_{20}ClF_2N_3O_3$ $[M+H]^+$: 508.1240; found, 508.1243.

Synthesis of ethyl 7-chloro-1-((1-(2-chlorobenzyl)-1H-benzo[d]imidazol-2-yl)methyl)-6-fluoro-4-oxo-1,4-dihydroquinoline-3-carboxylate (5d)

Compound **5d** was prepared according to the procedure for the preparation of compound **4a**, starting from compound **3** (2.284 g, 8.470 mmol), potassium carbonate (1.169 g, 8.470 mmol), sodium iodide (1.270 g, 8.470 mmol) and compound **10d** (2.513 g, 9.148 mmol). The pure product **5d** was obtained as white solid (1.892 g). Yield: 42.6%; mp: 220–221 °C; IR (KBr, cm^{-1}) v: 3049 (aromatic C–H), 2976, 2935, 2902 (CH_2, CH_3), 1898, 1730 (C=O), 1613, 1551, 1479, (aromatic frame); ^{1}H NMR (600 MHz, DMSO-d_6, ppm) δ 8.82 (s, quinolone-2-*H*, 1H), 8.16 (d, *J* = 5.8 Hz, quinolone-5-*H*, 1H), 7.94 (d, *J* = 9.2 Hz, quinolone-8-*H*, 1H), 7.67 (dd, *J* = 5.5, 3.3 Hz, benzimidazolyl-4-*H*, 1H), 7.44 (d, *J* = 8.0 Hz, benzimidazolyl-7-*H*, 1H), 7.42 (dd, *J* = 5.7, 3.2 Hz, ClPh-3-*H*, 1H), 7.22 (dt, *J* = 13.6, 6.7 Hz, ClPh-4,5,6-*H*, 3H), 6.92 (t, *J* = 7.5 Hz, benzimidazolyl-5-*H*, 1H), 6.12 (d, *J* = 7.6 Hz, benzimidazolyl-6-*H*, 1H), 6.05 (s, quinolone-1-NCH_2, 2H), 5.75 (s, benzimidazolyl-1-NCH_2, 2H), 4.23 (q, *J* = 7.0 Hz, COOCH_2, 2H), 1.29 (t, *J* = 7.1 Hz, COOCH$_2$CH_3, 3H); ^{13}C NMR (151 MHz, DMSO-d_6, ppm) δ 171.7 (*C*=O), 164.4 (O=*C*OCH$_2$CH$_3$), 155.6, 154.0, 150.9, 149.3, 142.2, 137.1, 136.3, 133.7, 131.9, 130.0, 129.7, 127.8, 126.8, 125.5, 123.8, 122.9, 120.8, 119.9, 112.9, 112.8, 111.1, 60.4, 50.2 (*C*H$_2$), 45.3, 14.8; ESI-MS (m/z): 524 $[M+H]^+$; HRMS (TOF) calcd. for $C_{27}H_{20}Cl_2FN_3O_3$ $[M+H]^+$: 524.0944; found, 524.0945.

Synthesis of ethyl 7-chloro-1-((1-(4-chlorobenzyl)-1H-benzo[d]imidazol-2-yl)methyl)-6-fluoro-4-oxo-1,4-dihydroquinoline-3-carboxylate (5e)

Compound **5e** was prepared according to the procedure for the preparation of compound **4a**, starting from compound **3** (2.356 g, 8.737 mmol), potassium carbonate (1.206 g, 8.737 mmol), sodium iodide (1.310 g, 8.737 mmol) and compound **10e** (2.544 g, 8.737 mmol). The pure product **5e** was obtained as white solid (1.764 g). Yield: 38.5%; mp: 208–209 °C; IR (KBr, cm^{-1}) v: 3081, 3053 (aromatic C–H), 2975, 2902 (CH_2, CH_3), 1884, 1722 (C=O), 1616, 1550, 1487, (aromatic frame); ^{1}H NMR (600 MHz, DMSO-d_6, ppm) δ 8.86 (s, quinolone-2-*H*, 1H), 8.03 (d, *J* = 9.2 Hz, quinolone-5-*H*, 1H), 7.98 (d, *J* = 5.9 Hz, quinolone-8-*H*, 1H), 7.58 (d, *J* = 8.0 Hz, benzimidazolyl-4-*H*, 1H), 7.51 (d, *J* = 8.1 Hz, benzimidazolyl-7-*H*, 1H), 7.36 (d, *J* = 8.4 Hz, ClPh-3,5-*H*, 2H), 7.24 (t, *J* = 7.6 Hz, benzimidazolyl-5-*H*, 1H), 7.19 (t, *J* = 7.6 Hz, benzimidazolyl-6-*H*, 1H), 7.14 (d, *J* = 8.5 Hz, ClPh-2,6-*H*, 2H), 6.03 (s, quinolone-1-NCH_2, 2H), 5.71 (s, benzimidazolyl-1-NCH_2, 2H), 4.24 (q, *J* = 7.1 Hz, COOCH_2, 2H), 1.28 (d, *J* = 7.1 Hz, COOCH$_2$CH_3, 3H); ^{13}C NMR (151 MHz, DMSO-d_6, ppm) δ 171.9 (*C*=O), 164.6 (O=*C*OCH$_2$CH$_3$), 155.7, 154.0, 151.3, 149.2, 142.3, 137.1, 136.3, 135.7, 132.9, 129.2, 128.9, 123.5, 122.6, 120.7, 119.8, 113.0, 112.8, 111.1, 110.9, 60.5, 49.9 (*C*H$_2$), 46.4, 14.7; ESI-MS (m/z): 524 $[M+H]^+$; HRMS (TOF) calcd. for $C_{27}H_{20}Cl_2FN_3O_3$ $[M+H]^+$: 524.0944; found, 524.0975.

Synthesis of ethyl 7-chloro-1-((1-(2,4-dichlorobenzyl)-1H-benzo[d]imidazol-2-yl)methyl)-6-fluoro-4-oxo-1,4-dihydroquinoline-3-carboxylate (5f)

Compound **5f** was prepared according to the procedure for the preparation of compound **4a**, starting from compound **3** (1.951 g, 7.235 mmol), potassium carbonate (0.998 g, 7.235 mmol), sodium iodide (1.084 g, 7.235 mmol) and compound **10f** (2.356 g, 7.235 mmol). The pure product **5f** was obtained as white solid (1.584 g). Yield: 39.2%; mp: 224–225 °C; IR (KBr, cm^{-1}) v: 3051 (aromatic C–H), 2978 (CH_2, CH_3), 1724, 1692 (C=O), 1612, 1551, 1485, (aromatic frame); ^{1}H NMR (600 MHz, DMSO-d_6, ppm) δ 8.82 (s, quinolone-2-*H*, 1H), 8.15 (d, *J* = 5.9 Hz, quinolone-5-*H*, 1H), 7.95 (d, *J* = 9.2 Hz, quinolone-8-*H*, 1H), 7.66 (dt, *J* = 6.5, 2.5 Hz, 2,4-Cl$_2$Ph-3-*H*, 1H), 7.60 (d, *J* = 2.1 Hz, benzimidazolyl-4-*H*, 1H), 7.48–7.43 (m, benzimidazolyl-7-*H*, 1H), 7.26–7.21 (m, benzimidazolyl-5,6-*H*, 2H), 7.03 (dd, *J* = 8.4, 2.1 Hz, 2,4-Cl$_2$Ph-5-*H*, 1H), 6.12 (d, *J* = 8.4 Hz, 2,4-Cl$_2$Ph-6-*H*, 1H), 6.03 (s, quinolone-1-NCH_2, 2H), 5.73 (s, benzimidazolyl-1-NCH_2, 2H), 4.24 (q, *J* = 7.1 Hz, COOCH_2, 2H), 1.30 (t, *J* = 7.1 Hz, COOCH$_2$CH_3, 3H); ^{13}C NMR (151 MHz, DMSO-d_6, ppm) δ 171.7 (C=O), 164.5 (O=*C*OCH$_2$CH$_3$), 155.7, 154.0, 150.9, 149.3, 142.2, 137.1, 136.3, 133.4, 132.9, 132.8, 129.5, 128.2, 128.0, 123.8, 122.9, 120.8, 120.0, 112.9, 112.7, 111.1, 110.9, 60.4, 50.2 (*C*H$_2$), 44.9, 14.8; ESI-MS (m/z): 580 $[M+Na]^+$; HRMS (TOF) calcd. for $C_{27}H_{20}Cl_2FN_3O_3$ $[M+Na]^+$: 580.0374; found, 580.0376.

Synthesis of ethyl 1-((1-allyl-1H-benzo[d]imidazol-2-yl)methyl)-7-chloro-6-fluoro-4-oxo-1,4-dihydro quinoline-3-carboxylate (6a)

Compound **6a** was prepared according to the procedure for the preparation of compound **4a**, starting from compound **3** (2.284 g, 8.470 mmol), potassium carbonate (1.169 g, 8.470 mmol), sodium iodide (1.270 g, 8.470 mmol) and compound **12a** (1.751 g, 8.470 mmol). The pure product **6a** was obtained as white solid (1.428 g). Yield: 38.3%; mp: 125–126 °C; IR (KBr, cm^{-1}) v: 3050 (aromatic C–H, CH=CH$_2$), 2980, 2935 (CH_2, CH_3), 1893, 1724 (C=O), 1614, 1550, 1486, (aromatic frame); ^{1}H NMR (600 MHz, $CDCl_3$, ppm) δ 8.57 (s, quinolone-2-*H*, 1H), 8.12 (d, *J* = 8.9 Hz, quinolone-5-*H*, 1H), 7.83 (d, *J* = 5.5 Hz, quinolone-8-*H*, 1H), 7.74–7.68 (m, benzimidazolyl-4-*H*, 1H), 7.33–7.29 (m, benzimidazolyl-7,5-*H*, 2H), 7.28 (d, *J* = 9.5 Hz, benzimidazolyl-6-*H*, 1H), 5.97–5.88 (m, CH$_2$C*H*=CH$_2$, 1H), 5.58 (s, quinolone-1-NCH_2, 2H), 5.21 (t, *J* = 11.8 Hz, CH$_2$CH=C*H*$_2$, 1H), 4.86 (t, *J* = 18.9 Hz, CH$_2$CH=CH_2, CH_2CH=CH$_2$, 3H), 4.33 (q, *J* = 7.0 Hz, COOCH_2, 2H), 1.36 (t, *J* = 7.0 Hz, COOCH$_2$CH_3, 3H); ^{13}C NMR (151 MHz, $CDCl_3$, ppm) δ 172.8 (*C*=O), 164.8 (O=*C*OCH$_2$CH$_3$), 156.4, 154.8, 149.8, 146.1, 142.2, 136.1, 135.7, 131.1, 124.0, 123.0, 120.4, 120.3, 119.2, 118.0, 113.9, 111.4, 109.7, 61.0, 51.3 (CH$_2$), 46.1, 14.4; ESI-MS (m/z): 440 $[M+H]^+$; HRMS (TOF) calcd. for $C_{23}H_{20}ClFN_3O_3$ $[M+H]^+$: 440.1177; found, 440.1201.

Synthesis of ethyl 7-chloro-6-fluoro-4-oxo-1-((1-(prop-2-yn-1-yl)-1H-benzo[d]imidazol-2-yl)methyl)-1,4-dihydroquinoline-3-carboxylate (6b)

Compound **6b** was prepared according to the procedure for the preparation of compound **4a**, starting from compound **3** (3.058 g, 11.340 mmol), potassium carbonate (1.565 g, 11.340 mmol), sodium iodide (1.670 g, 11.340 mmol) and compound **12b** (2.321 g, 11.340 mmol). The pure product **6b** was obtained as white solid (1.226g). Yield: 24.7%; mp: 181–182 °C; IR (KBr, cm^{-1}) v: 3293 (C≡CH), 3057 (aromatic C–H), 2962, 2904 (CH_2, CH_3), 2120 (C≡C), 1906, 1732 (C=O), 1614, 1552, 1481 (aromatic frame); ^{1}H NMR (600 MHz, DMSO-d_6, ppm) δ 8.95 (s, quinolone-2-*H*, 1H), 8.06 (d, *J* = 4.0 Hz, quinolone-5-*H*, 1H), 7.69 (d, *J* = 3.8 Hz, quinolone-8-*H*, benzimidazolyl-4-*H*, 2H), 7.53 (s, benzimidazolyl-7-*H*, 1H), 7.29 (d, *J* = 5.2 Hz, benzimidazolyl-6-*H*, 5-H), 7.19 (s, benzimidazolyl-6-*H*, 1H), 6.06 (s, quinolone-1-NCH_2, 2H), 5.36 (s, CH_2C≡CH, 2H), 4.25 (q, *J* = 5.6 Hz, COOCH_2CH$_3$, 2H), 3.53 (s, CH$_2$C≡C*H*, 1H), 1.29 (t, *J* = 2.5 Hz, COOCH$_2$CH_3, 3H); ^{13}C NMR (151 MHz, DMSO-d_6, ppm) δ 172.9 (*C*=O), 164.6 (O=*C*OCH$_2$CH$_3$), 156.1, 154.5, 150.1, 148.9, 142.2, 137.2, 135.6, 129.1, 123.4, 122.7, 120.7, 118.6, 113.1, 112.5, 110.9, 78.3 (*C*≡CH), 76.9 (C≡*C*H), 60.5, 50.5 (*C*H$_2$), 31.1, 14.8; ESI-MS (m/z): 438 $[M+H]^+$; HRMS (TOF) calcd. for $C_{23}H_{17}ClFN_3O_3$ $[M+H]^+$: 438.1021; found, 438.1020.

Acknowledgements

This work was partially supported by National Natural Science Foundation of China (Nos. 21672173) and Chongqing Special Foundation for Postdoctoral Research Proposal (No. Xm2017184).

Keywords: Quinolone • Benzimidazole • Antibacterial • Antifungal • DNA

References:

[1] a) D. Szamosvári, T. Böttcher, *Angew. Chem. Int. Ed.* **2017**, *56*, 7271–7275; b) S. F. Cui, D. Addla, C. H. Zhou, *J. Med. Chem.* **2016**, *59*, 4488–4510.

[2] a) X. F. Zou, L. Zhang, Z. J. Wang, Y. Luo, *J. Am. Chem. Soc*. **2016**, *138*, 2064–2077; b) Y. Cheng, S. R. Avula, W. W. Gao, D. Addla, V. K. R. Tangadanchu, L. Zhang, J. M. Lin, C. H. Zhou, *Eur. J. Med. Chem.* **2016**, *124*, 935–945.

[3] a) W. A. Velema, J. P. van der Berg, M. J. Hansen, W. Szymanski, A. J. M. Driessen, B. L. Feringa, *Nat. Chem.* **2013**, *5*, 924–928; b) X. M. Peng, G. L. V. Damu, C. H. Zhou, *Curr. Pharm. Des*. **2013**, *19*, 3884–3930.

[4] L. Zhang, K. V. Kumar, S. Rasheed, S. L. Zhang, R. X. Geng, C. H. Zhou, *Med. Chem. Commun*. **2015**, *6*, 1303–1310.

[5] W. D. Hong, P. D. Gibbons, S. C. Leung, R. Amewu, P. A. Stocks, A. Stachulski, P. Horta, M. L. S. Cristiano, A. E. Shone, D. Moss, A. Ardrey, R. Sharma, A. J. Warman, P. T. P. Bedingfield, N. E. Fisher, G. Aljayyoussi, S. Mead, M. Caws, N. G. Berry, S. A. Ward, G. A. Biagini, P. M. O'Neill, G. L. Nixon, *J. Med. Chem.* **2017**, *60*, 3703–3726.

[6] F. Wang, L. Jin, L. H. Kong, X. W. Li, *Org. Lett.* **2017**, *19*, 1812–1815.

[7] S. F. Cui, L. P. Peng, H. Z. Zhang, S. Rasheed, K. V. Kumar, C. H. Zhou, *Eur. J. Med. Chem.* **2014**, *86*, 318–334.

[8] a) L. Zhang, K. V. Kumar, R. X. Geng, C. H. Zhou, *Bioorg. Med. Chem. Lett*. **2015**, *25*, 3699–3705; b) X. M. Peng, G. X. Cai, C. H. Zhou, *Curr. Top. Med. Chem.* **2013**, *13*, 1963–2010.

[9] a) L. Zhang, K. V. Kumar, S. Rasheed, R. X. Geng, C. H. Zhou, *Chem. Biol. Drug. Des.* **2015**, *86*, 648–655; b) W. W. Gao, S. Rasheed, V. K. R. Tangadanchu, Y. Sun, X. M. Peng, Y. Cheng, F. X. Zhang, J. M. Lin, C. H. Zhou, *Sci. China Chem.* **2017**, *60,* 769–785.

[10] T. S. Crofts, A. J. Gasparrini, G. Dantas, *Nat. Rev. Microbiol*. **2017**, *15*, 422–434.

[11] K. Y. Yeong, A. A. Mohamed, C. W. Ang, N. S. Amir, P. Keykavous, S. C. Tan, *Eur. J. Med. Chem.* **2014**, *83*, 448–454.

[12] L. Zhang, D. Addla, J. Ponmani, A. Wang, D. Xie, Y. N. Wang, S. L. Zhang, R. X. Geng, G. X. Cai, S. Li, C. H. Zhou, *Eur. J. Med. Chem.* **2016**, *111*, 160–182.

[13] S. F. Cui, Y. Ren, S. L. Zhang, X. M. Peng, G. L. V. Damu, R. X. Geng, C. H. Zhou, *Bioorg. Med. Chem. Lett*. **2013**, *23*, 3267–3272.

[14] a) H. Z. Zhang, J. Ponmani, K. V. Kumar, C. H. Zhou, *New J. Chem.* **2015**, *39*, 5776–5796; b) K. Y. Yeong, A. A. Mohamed, C. W. Ang, S. C. Tan, I. Rusli, *Eur. J. Med. Chem.* **2015**, *93*, 614–624.

[15] J. Ponmani, L. Zhang, S. R. Avula, C. H. Zhou, *Eur. J. Med. Chem.* **2016**, *122*, 205–215.

[16] L. T. Wu, Z. Jiang, J. J Shen, H. Yi, Y. C. Zhan, M. Q. Sha, Z. Wang, S. T. Xue, Z. R. Li, *Eur. J. Med. Chem.* **2016**, *114*, 328–336.

[17] D. Song, S. T. Ma, *ChemMedChem.* **2016**, *11*, 646–659.

[18] H. Z. Zhang, S. F. Cui, S. Nagarajan, S. Rasheed, G. X. Cai, C. H. Zhou, *Tetrahedron Lett*. **2014**, *55*, 4105–4109.

[19] N. S. El-Gohary, M. I. Shaaban, *Eur. J. Med. Chem.* **2017**, *137*, 439–449.

[20] W. A. Velema, J. P. van der Berg, W. Szymanski, A. J. M. Driessen, B. L. Feringa, *ACS Chem. Biol*. **2014**, *9*, 1969–1974.

[21] H. T. Bai, H. Y. Zhang, R. Hu, H. Chen, F. T. Lv, L. B. Liu, S. Wang, *Langmuir* **2017**, *33*, 1116–1120.

[22] a) H. Z. Zhang, S. C. He, Y. J. Peng, H. J. Zhang, L. Gopala, V. K. R. Tangadanchu, L. L. Gan, C. H. Zhou, *Eur. J. Med. Chem.* **2017**, *136*, 165–183; b) X. J. Fang, J. Ponmani, S. R. Avula, Q. Zhou, C. H. Zhou, *Bioorg. Med. Chem. Lett.* **2016**, *26*, 2584–2588; c) Y. L. Luo, K. Baathulaa, V. K. Kannekanti, C. H. Zhou, G. X. Cai, *Sci. China Chem.* **2015**, *58*, 483–494.

[23] X. F. Fang, D. Li, V. K. R. Tangadanchu, L. Gopala, W. W. Gao, C. H. Zhou, *Bioorg. Med. Chem. Lett*. **2017**, *27*, 4964–4969.

[24] a) R. P. Tayade, N. Sekar, *Dyes Pigments* **2016**, *128*, 111–123; b) H. B. Liu, W. W. Gao, V. K. R. Tangadanchu, C. H. Zhou, R. X. Geng, *Eur. J. Med. Chem.* **2018**, *143*, 66–84.

[25] L. Zhang, X. M. Peng, G. L. V. Damu, R. X. Geng, C. H. Zhou, *Med. Res. Rev.* **2014**, *34*, 340–437.

[26] a) X. M. Peng, L. P. Peng, S. Li, S. R. Avula, K. V. Kumar, S. L. Zhang, K. Y. Tam, C. H. Zhou, *Future Med. Chem.* **2016**, *8,* 1927–1940; b) N. S. El-Gohary, M. I. Shaaban, *Eur. J. Med. Chem.* **2017**, *131*, 255–262.

[27] W. W. Gao, C. H. Zhou, *Future Med. Chem.* **2017**, *9*, 1461–1464.

[28] H. Z. Zhang, G. L. V. Damu, G. X. Cai, C. H. Zhou, *Curr. Org. Chem.* **2014**, *18*, 359–406.

[29] a) M. Z. Hernandes, S. M. T. Cavalcanti, D. R. M. Moreira, W. F. de Azevedo Junior, A. C. L. Leite, *Curr. Drug Targets* **2010**, *11*, 303–314; b) G. Cavallo, P. Metrangolo, R. Milani, T. Pilati, A. Priimagi, G. Resnati, G. Terraneo, *Chem. Rev*. **2016**, *116*, 2478–2601.

[30] a) J. Kang, V. K. R. Tangadanchu, L. Gopala, W. W. Gao, Y. Cheng, H. B. Liu, R. X. Geng, S. Li, C. H. Zhou, *Chin. Chem. Lett*. **2017**, *28*, 1369–1374; b) C. H. Zhou, Y. Wang, *Curr. Med. Chem.* **2012**, *19*, 239–280.

[31] Q. C. Cao, H. Wang, V. K. R. Tangadanchu, L. Gopala, G. X. Cai, C. H. Zhou, *Sci. Sin. Chim.* **2017**, *47*, 844–858.

[32] L. P. Peng, S. Nagarajan, S. Rasheed, C. H. Zhou, *Med. Chem. Commun*. **2015**, *6*, 222–229.

[33] H. H. Gong, K. Baathulaa, J. S. Lv, G. X. Cai, C. H. Zhou, *Med. Chem. Commun.* **2016**, *7*, 924–931.

[34] J. Ponmani, H. B. Liu, L. Gopala, Y. Cheng, X. M. Peng, R. X. Geng, C. H. Zhou, *Bioorg. Med. Chem. Lett.* **2017**, *27*, 1737–1743.

[35] H. H. Gong, D. Addla, J. S. Lv, C. H. Zhou, *Curr. Top. Med. Chem.* **2016**, *16*, 3303–3364.

[36] G. S. Bisacchi, *J. Med. Chem.* **2015**, *58*, 4874–4882.

[37] R. I. Al-Wabli, A. R. Al-Ghamdi, H. A. Ghabbour, M. H. Al-Agamy, J. C. Monicka, I. H. Joe, M. I. Attia, *Molecules* **2017**, *22*, 373–389.

[38] a) Y. Zhang, G. L. V. Damu, S. F. Cui, J. L. Mi, V. K. R. Tangadanchu, C. H. Zhou, *Med. Chem. Commun*. **2017**, *8*, 1631–1639; b) Z. Z. Li, L. Gopala, V. K. R. Tangadanchu, W. W. Gao, C. H. Zhou, *Bioorg. Med. Chem.* **2017**, *25*, 6511–6522.

[39] a) B. T. Yin, C. Y. Yan, X. M. Peng, S. L. Zhang, S. Rasheed, R. X. Geng, C. H. Zhou, *Eur. J. Med. Chem.* **2014**, *71*, 148–159; b) W. W. Gao, L. Gopala, R. R. Y. Bheemanaboina, G. B. Zhang, S. Li., C. H. Zhou, *Eur. J. Med. Chem.* **2018**, *146*, 15–37.

[40] a) N. Shahabadi, N. H. P. Moghadam, *J. Lumin*. **2013**, *134*, 629–634; b) G. W. Zhang, P. Fu, L. Wang, M. M. Hu, *J. Agric. Food Chem.* **2011**, *59*, 8944–8952.

[41] N. Sabine, S. Katrin, G. R. Sebastian, M. Magnus, K. Markus, D. Sandra, M. Andrea, S. Jens, H. Georg, B. Knut, H. Ulrike, S. S. Jurgen, *J. Med. Chem.* **2009**, *52*, 4257–4265.

[42] D. Xue, Y. Q. Long, *J. Org. Chem.* **2014**, *79*, 4727–4734.

Entry for the Table of Contents

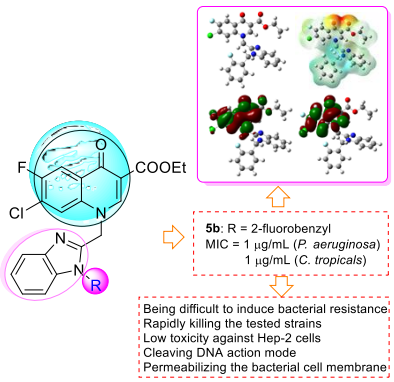

A series of new benzimidazole quinolone hybrids as cleaving agents towards drug-resistant *P. aeruginosa* DNA were prepared and evaluated on their antimicrobial activities *in vitro* by changing substituents at of nitrogen atom of benzimidazole ring and investigating their influence on antimicrobial activity. Notably, 2-fluorobenzyl derivative **5b** showed remarkable antimicrobial activities against the resistant *P. aeruginosa* and *C. tropicalis* isolated from infected patients.